

EFFECT OF CLAY PARTICLES SIZE AND LOCATION ON COALESCENCE IN PMMA/PS BLENDS

Julie GENOYER^{1,2}, Nicole R. DEMARQUETTE^{2*}, and Jérémie SOULESTIN^{1*}

¹ *IMT Lille Douai, Department of Polymers and Composites Technology & Mechanical Engineering, Douai, France*

² *École de technologie supérieure, Department of Mechanical Engineering, Montreal, QC H3C 1K3, Canada*

Abstract

The addition of 6 different clays (laponite, montmorillonite, halloysite and their organomodified counterparts) to poly(methyl methacrylate) (PMMA), polystyrene (PS) and their blends was studied. The morphologies of the obtained composites were studied using transmission electron microscopy (TEM) and scanning electron microscopy (SEM). Small angle oscillatory shear (SAOS) experiments, as well as, shear induced coalescence tests were carried out to evaluate the role of the clay as a coalescence inhibitor. Using the six different clays enabled the evaluation of the effect of clay location and clay platelet size for a given location (matrix, dispersed phase, interphase) on the coalescence phenomenon. A decrease of the dispersed phase of the blend was generally observed upon the addition of clay. Clays located exclusively in the matrix (laponite, montmorillonite, halloysite and modified halloysite) were shown to migrate to the interface during coalescence tests, inducing a decrease of coalescence at a certain extent of migration. Modified montmorillonite, located at the interface, was the most efficient clay at inhibiting coalescence, due to relaxation of Marangoni stresses with an important barrier effect. Overall, it was shown that having a certain size of a nanoparticle is essential for it to locate at the interface and inhibit coalescence. Nanoparticles with a larger size than the droplets are not able to locate at the interface and therefore, do not have an effect on coalescence. Conversely, nanoparticles whose size is 10 % or less of the droplet, were found to be well dispersed in the whole blend. These particles did not have a preferred location nor had an effect on coalescence.

Introduction

Most of the commercial plastics products consist of blends of immiscible polymers. These multiphase materials are interesting as one can control their properties by controlling their morphology, which in turn can be controlled during processing. When subjected to flow during processing, polymer blends' morphology is influenced by breakup and coalescence

phenomena. In the case of a blend with a dispersed droplet shape morphology subjected to uniform steady shear flow, the deformation of a droplet, leading to breakup or coalescence, depends on the capillary number (1) and the viscosity ratio (2) defined by

$$Ca = \frac{F_{viscous}}{F_{interfacial}} = \frac{\eta_m \dot{\gamma} R_v}{\alpha} \quad (1)$$

$$p = \frac{\eta_d}{\eta_m} \quad (2)$$

Where η_m and η_d are the viscosities of the matrix and the droplets, respectively, $\dot{\gamma}$ is the shear rate, R_v is the volume average radius of the droplets, and α is the interfacial tension.

The capillary number Ca is the ratio of the viscous forces over the interfacial forces. Above a critical value of the capillary number, Ca_c , the drops will break up, and below it, coalescence is likely to occur when the average droplets radius is smaller than a critical value [1]. With an average droplet size smaller than the critical value and a shear rate lower than the critical shear rate, coalescence is likely to occur until a steady state is reached. To do so, many authors such as Vinckier et al. [2], used a pre-shear at high shear rate to generate a fine morphology and then lowered the shear rate in step to below a critical value to be able to observe coalescence only.

Controlling the morphology can be achieved adding compatibilizers. A classic compatibilizer can be a premade block copolymer or a copolymer created in-situ by an interfacial reaction [3], [4]. Alternatively, it was found that nanoparticles can serve as efficient compatibilizers if they are organo-modified previously by either chemical grafting [5]–[7] or ionic exchange [8]–[11]. Such modification enables a better dispersion and a better compatibility with the polymers involved. For example, montmorillonite, a smectic clay, has been used as a compatibilizer for several polymer blends. Montmorillonite is a layered silicate composed of two siloxane tetrahedral sheets sandwiching an aluminum octahedral sheet. The silicate layers are negatively charged, which is counterbalanced by exchangeable cations such as Na^+ and Ca^{2+} placed in the interlayer. When montmorillonite is used with polymers, the interlayer cations are usually exchanged with quaternary ammonium salts to increase the basal spacing and enhance the compatibility with the polymeric matrix [8], [12].

Laponite is less commonly used as a compatibilizer or filler. It is a synthetic clay shaped in discs of around 30 nm in diameter [13] which has the same chemical structure as montmorillonite. The same organic modification can be carried out for laponite. The only difference is that laponite has a smaller Cation Exchange Capacity (CEC) than montmorillonite. Values of laponite's CEC found in the literature range between 47 and 75 meq/100 g [14]–[16], whereas, montmorillonite's CEC is of 92.5 meq/100g. Montmorillonite has been used more extensively than laponite for polymer blend compatibilization Yurekli et al. [17] studied the effect of these two clays on phase separation morphology. They concluded that both clays slowed down the phase separation.

Another type of clay, halloysite, which is composed of natural rod nanoparticles of 50 to 5000 nm length and of 20 to 200 nm outer diameter, are starting to get some interest in the development of nanocomposites [18]. Halloysite's chemistry is similar to the one of the other clays mentioned above. Its geometry, however, is quite different. In this case, the silicate sheet is rolled into cylinders, the outside layer of the which is made of SiO₂ and is negatively charged, whereas, the Al(OH)₃ inner lumen is positively charged. Thanks to this difference in the external and internal chemical composition, a selective modification is possible: cations can be adsorbed around the nanoparticles whereas anions would preferably place themselves inside the tube [19]. Halloysite has attracted attention for several applications, for instance as natural nanocontainer for loading and sustained release of chemical agents [19]. To our knowledge, the only study on the use of halloysites as compatibilizers was reported by Pal et al. [20], who studied the influence of adding halloysites in a blend of polyoxymethylene/polypropylene. They found that the presence of halloysites induced a reduction in the droplet size. They also were able to show that modified halloysites had more effect than the pure unmodified ones. We decided to employ halloysite as a compatibilizer.

Generally, upon addition of a compatibilizer and irrespective of its chemical nature, one or several of the following phenomena can be observed in the case of a blend with a droplet dispersion type morphology: reduction of the droplet size [21], [22], inhibition of droplet's coalescence [23]–[27], decrease in interfacial tension [28]–[32], and presence of an additional relaxation phenomenon [28], [32]–[40]. The additional relaxation phenomenon observed upon addition of compatibilizers is known to correspond to the relaxation of Marangoni stresses induced by a non-homogeneous concentration of compatibilizers at the interface [34], [39]–[41]. Indeed, when two droplets approach each other, the matrix layer between them is squeezed out, dragging some of the compatibilizer around the interface with it. A gradient in

compatibilizer concentration on the surface of the droplets results from this, causing what we call Marangoni stresses to appear. Those stresses make the compatibilizer redistribute itself evenly on the surface, thereby preventing coalescence and creating the relaxation described previously. This was elegantly proved in the case of block copolymer by Jeon and Macosko [41] who visualized fluorescent PS-PMMA block copolymer concentration gradients, during flow at the surface of a PMMA droplet in a PS matrix. However, Genoyer et al. [42] showed that in the case of block copolymers, Marangoni stresses alone cannot prevent coalescence. Indeed, the molar mass of the block copolymer must be high enough to induce steric hindrance as well, or else coalescence is not affected [42]. It was also shown using rheology that Marangoni stresses can also appear in the case of clay nanoplatelets [40], however, up to the time this work was done, no one has shown that Marangoni effect solely is responsible for the decrease of coalescence in polymer blends with nanoparticles.

The morphology, the interfacial tension, and the relaxation phenomena in the blends can be inferred from rheological characterization in the linear viscoelastic regime. Small amplitude oscillatory shear (SAOS) experiments can reveal an increase in elasticity at low frequencies, resulting in a shoulder on the storage modulus curve as a function of frequency. The relaxation of the shape of the droplets (τ_F) is responsible for this increase [43]. In the case of compatibilized blends, an additional relaxation time (τ_β) may be observed, corresponding to the relaxation induced by Marangoni stresses [34]. However, in the case of dilute systems, those shoulders are so subtle that it is difficult to identify them visually. Obtaining the relaxation spectra by the method of Honerkamp and Weese [44] from SAOS data can be used to identify the different relaxations. Indeed, those spectra were found to clearly display the polymer chain relaxation, the droplet's shape relaxation, and the relaxation due to the rearrangement of compatibilizers at the interface, referred to as Marangoni's relaxation in this work.

Relaxations can also be studied using existing rheological models, which link the rheological behavior of polymer blends to their morphology. One such model is Palierne's model, which predicts the rheological behavior of a blend formed by two viscoelastic polymers in the linear viscoelastic regime [45]. An important approximation of this model assumes that the polymers should be viscous enough to render bulk forces such as gravitation and inertia negligible. Another approximation is that the emulsion should be monodispersed and diluted.

Several authors used and simplified the model to obtain a simple expression of droplet's shape relaxation time as follows [46]:

$$\tau_F = \frac{\left(\frac{R_v \eta_M}{4\alpha}\right) (19p + 16)(2p + 3 - 2\Phi(p - 1))}{10(p + 1) - 2\Phi(5p + 2)} \quad (3)$$

where R_v is the volume average droplet radius, α is the interfacial tension, p is the viscosity ratio, Φ is the volume fraction of the dispersed phase and η_M is the viscosity of the matrix.

In this work, the effect of addition of clay nanoparticles on the morphology and on the coalescence phenomenon of PMMA/PS blends was studied. PMMA/PS blends were used since they have a very well-known rheological behavior and hence allow to clearly identify additional phenomena induced by a compatibilizer. The morphology of the blends and the location of clay were assessed. Using six different clays enabled the evaluation of the effect of clay platelet size for a same location, as well as, the effect of clay location (matrix, dispersed phase, interphase) on coalescence phenomenon. The linear rheology results combined with Palierne's model were used to determine the evolution of the droplet shape and size during shear induced coalescence, as well as, witnessing the relaxation induced by Marangoni stresses in the case of clays at the interface.

A. Materials and methods

1. Materials

Poly(methylmethacrylate) (PMMA) PLEXIGLAS, grade 6N from Evonik, and polystyrene (PS) from INEOS Styrenics, grade EMPERA 350N, were used for this study. 3 different clays were used: Cloisite Na⁺ from Southern Clay Products (named here MMT), Laponite RD (L) from BYK Additives, and Halloysite (H) from Gelest Inc. The clays were organically modified using di(hydrogenated tallow)dimethylammonium chloride, Arquad 2HT-75, purchased from Sigma Aldrich.

The characteristics of the materials are reported in TABLE I and TABLE II.

TABLE I Properties of the polymers

Polymer	Density (g/cm ³)	Viscosity (η_0) (Pa.s) at 200 °C
PMMA	1.19	12,000
PS	1.04	9,800

TABLE II Properties of clays

Clay	Shape	Size	Surface area (m ² /g)	Cation exchange capacity (meq/100 g)
MMT	platelets	150-250 nm*	750	92.6
L	discs	25-30 nm D*	370	55
H	tubular	0.1-1.5 μm length, 10-200 nm OD**	64	8

*from the supplier

**measured using TEM pictures

2. Modification of clays

Neat clays were modified using the above mentioned surfactant in order to improve their affinity with polymers. The modification was done by ionic exchange at 60 % of the CEC. Infrared spectra showed a shift in the CH₂ antisymmetric stretching vibration and confirmed that the surfactants molecules interact with the clays surface [12]. XRD patterns allowed the verification of the intercalation of the surfactant by showing a larger basal spacing for mMMT and mL than their non-modified counterparts. XRD cannot be used in the case of halloysite as the surfactant is expected to localize itself at the surface, around the particle. Before each use, the clays were re-dried at 85 °C for at least 12 hours. In this paper, the modified clays are designated as mMMT, mL and mH.

3. Blending

A concentration of 10 % of dispersed phase was chosen as it would result in a droplet dispersion type morphology enabling the use of Palierne model that was derived for dilute systems. 90/10 blends of PMMA/PS to which 0 to 1 % of clay was added were prepared. All the percentages in this paper are weight percentages although volume concentrations were used for the calculations.

A micro twin screw extruder HAAKE MiniLab II from Thermo Scientific was used to prepare the blends. The extrusion was carried out at 200 °C and 50 rpm. Prior to mixing, PMMA was dried at 85 °C for at least 12 hours. The processing took place in two steps: first, the clays were mixed with the minor phase (PS) in direct extrusion mode, and then, PS+clay was mixed with PMMA for 7 minutes in cycle extrusion mode for 7 minutes. The aim was to follow the same procedure as in a previous study [40]. In the case of PMMA/PS blends without clay, the

minor phase was processed twice to undergo the same thermomechanical history as the blends with nanoparticles. This blend is called “Pure” in the rest of the paper.

Nanocomposites of PMMA and PS were also obtained. PMMA to which 0 to 5 % of clays was added, were extruded for 7 min in cycle extrusion mode. PS to which 0 to 10% clay was added nanocomposites were first extruded in direct extrusion mode and then for 7 min in cycle mode in order to undergo the same thermomechanical treatment as the dispersed phase in the blend. The differences in concentration of clay within the respective polymers stems from the fact that 90/10 blends were used.

4. Characterizations

Samples for rheological and morphological analyzes were molded into discs of 25 mm diameter and 1 mm thickness at 200 °C under 10 MPa for 10 minutes using a compression molding press.

The morphology was characterized by scanning electron microscopy (SEM) under high vacuum with a Hitachi S-4300SE/N SEM or a JEOL JCM-600 Plus. The samples were fractured at ambient temperature and coated with gold. The morphology was quantified with ImageJ software by considering at least 1000 particles for each sample. The volume average radii, which can be obtained using equation (4), are reported in this paper. The Paine model [47], [48] was used to identify a critical number of droplets to be measured to have a representative average radius. This critical number, N_{crit} , is a function of the width of the distribution and the geometric standard deviation (GSD) as described in equation (5). It led to a critical number ranging from 72 to 1420 depending on the sample. For a number of droplets measured above N_{crit} , the error can be estimated using equation (6) [47]. The vertical error bars on the $R_{v,SEM}$ values reported in the paper are the error estimated using Paine model.

$$R_{v,SEM} = \frac{\sum_i R_i^4}{\sum_i R_i^3} \quad (4)$$

$$N_{crit} = \exp (1.5 + 5.5 \ln(GSD) + 7.5 \ln^2(GSD)) \quad (5)$$

$$e = \frac{\ln(GSD) \exp (1.5 \ln(GSD) + 2.5 \ln^2(GSD))}{\sqrt{N}} \quad (6)$$

In order to obtain TEM pictures of blends containing non-modified clays, the samples were sectioned at room temperature with a thickness of ≈ 90 nm with the Leica Microsystems UCT ultramicrotome and transferred onto 200-mesh Cu TEM grids with a carbon supported film. The images were collected on the FEI TECNAI G² F20 S/TEM at an accelerating voltage of 200 kV.

Blends with modified clays samples for transmission electron microscopy were sectioned at room temperature at a thickness of ≈ 70 nm using a LEICA EM UC7 ultramicrotome and transferred to TEM grids with carbon supported film. The images were taken using a FEI TECNAI G² LAB6 at an accelerating voltage of 200 kV.

Linear rheology experiments were performed using two controlled stress rheometers: MCR 501 and MCR 302 from Anton Paar under dry nitrogen atmosphere. The results of the two rheometers were shown to corroborate within 5%. A parallel-plate geometry was used with a gap size of 0.9 mm and plate diameter of 25 mm. Thermal stability of the sample was checked by performing time sweep tests. It was shown that PMMA/PS blends were stable under nitrogen atmosphere for at least 2 hours at 200 °C. The linear viscoelastic region was defined by carrying out strain sweep tests. Finally, dynamic frequency sweep tests were performed for all blends and pure polymers at 200 °C and 220 °C at 4 % of strain. The frequency range was chosen to be from 300 to 0.01 Hz. The zero-shear viscosities of the neat polymers were determined using the curve of complex viscosity (Pa.s) versus frequency (rad/s) obtained from dynamic frequency sweep tests. Rheological experiments were shown to be reproducible within 5 %.

Shear induced coalescence tests were carried out on a MCR 302 at 200 °C under nitrogen atmosphere. The design of those tests is described in a previous paper [42] and reported in FIG 1. In this case, the critical capillary number, calculated using the experimental fit of Grace's curve by De Bruijn [49], is of 0.47. Thus, the critical shear rate is of 0.12 s⁻¹. Consequently, a constant shear rate of 0.05 s⁻¹, corresponding to a value below the critical capillary number, was chosen to ensure coalescence conditions. The coalescence tests were designed as described in Genoyer et al's work [42] with a succession of steady shear (shear induced coalescence) and frequency sweeps, as can be seen in FIG 1, to probe the evolution of morphology as first described in Vinckier et al.'s work [2]. Those tests last 10 hours in total. The rheological behavior was then evaluated as a function of strain ((time length of steady shear)*(shear rate)). A decrease in the complex viscosity could be observed over time during this test. To take this into consideration, calculations were done considering the decrease of pure PMMA and pure PS complex viscosity at each strain. This data was obtained by running

This is the author's peer reviewed, accepted manuscript. However, the online version of record will be different from this version once it has been copyedited and typeset.
PLEASE CITE THIS ARTICLE AS DOI: 10.1122/1.5102177

the same test on pure polymers. As such, at each step, different PMMA and PS viscosities were taken into account in order to calculate the radius of the droplets. As it might not take fully into account the total degradation of the blends, which may be influenced by the presence of particles, the droplets' size was measured after shear induced coalescence test and compared to the calculated $R_{v,P}$. The results of both methods were in good agreement (see FIG 2).

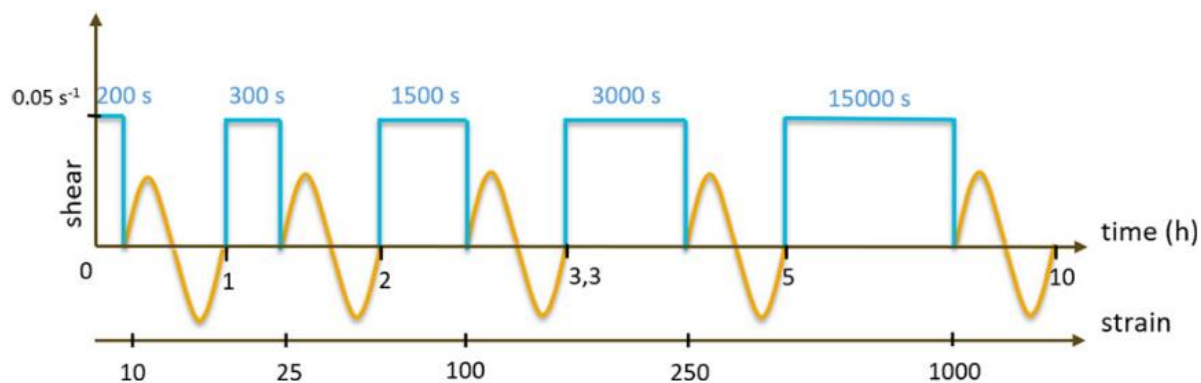


FIG 1 Design of coalescence experiments [42]

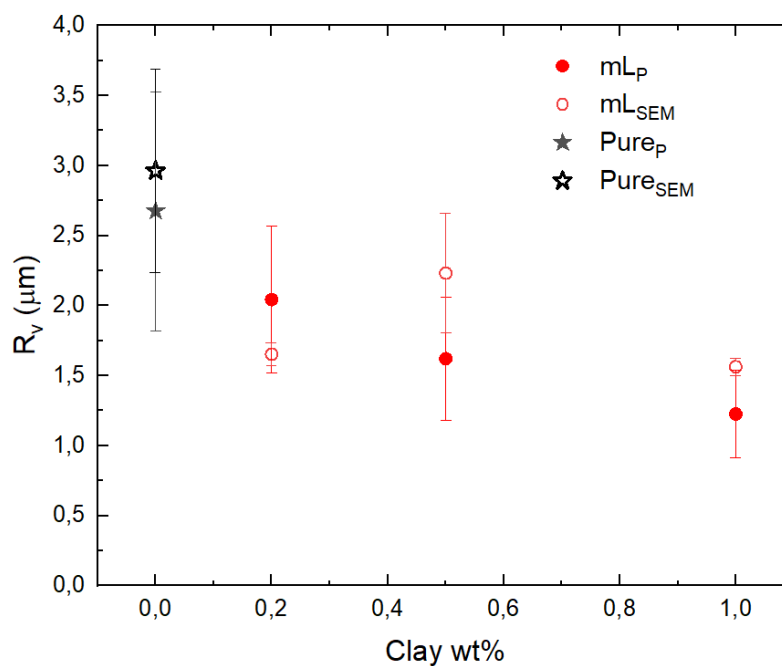


FIG 2 Volume average radii of pure blend and blends containing mL after coalescence test obtained by Palierne's model (P) and by SEM

B. Results and discussion

The modified and neat clays were added to PMMA/PS blends. The location of the nanoparticles was observed using TEM. It can be seen in FIG 3 that there are three possible

location: in the whole blend (FIG 3a), at the interface (FIG 3b), and in the matrix (FIG 3c, d, e and f).

mH, L, MMT and H are all located in the matrix because those nanoparticles, or aggregates of nanoparticles, are too big to locate at the interface. As the particles have different sizes, the first part of the results will focus on the addition of mH, L, MMT and H to study the effect of the size of the particles on coalescence.

mL, mMMT and mH all have different locations because of the size of the considered nanoparticles. mL nanoparticles are so small that they can disperse easily in the whole blend, mMMT which have a size of the order of magnitude of the radius of the droplets prefer to locate themselves at the interface, and mH are too big to locate anywhere else than the matrix. As such, the second part of this study will focus on the effect of location of clay nanoparticles on the compatibilization mechanism and more specifically on the coalescence phenomenon.

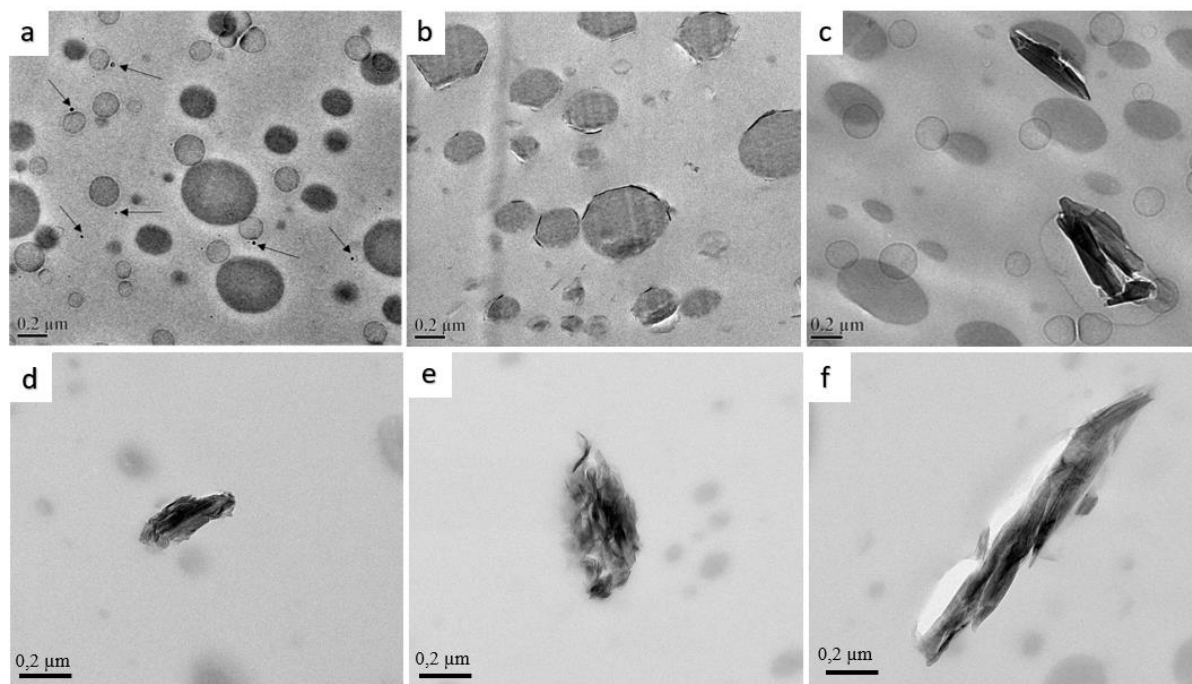


FIG 3 TEM pictures of PMMA/PS blends with 1 % of (a) mL, (b) mMMT, (c) mH, (d) L, (e) MMT and (f) H.

1. Effect of the size of particles located within the matrix

First, the effect of the size of the nanoparticles on the compatibilization mechanism of the blend and more particularly on the coalescence phenomenon was studied. To do so the 3 neat clays, MMT, L and H and one modified clay, mH, were used. As it can be seen in FIG 3d, e and f, all the neat clays are aggregated due to their poor affinity with the polymers and are located in the matrix. mH is better dispersed due to its organic modification, however, it is also

located in PMMA because of its large size. According to TEM observations such as the ones shown in FIG 3, the size of aggregates or nanoparticles are as follows: $L \leq mH < MMT < H$.

The morphology of PMMA/PS blends to which clays were added was observed and quantified using SEM. FIG 4 shows that adding clays results in a decrease of the droplet size. The results obtained are similar for each clay, indicating that the size of the clay particles does not have a noticeable influence on the size of the dispersed droplet obtained after processing. As the clays are not located at the interface, the decrease of the dispersed droplet size cannot be due to a decrease in interfacial tension as usually found. However, due to the large size of the aggregates it may be due a modification of the rheological properties of the PMMA matrix.

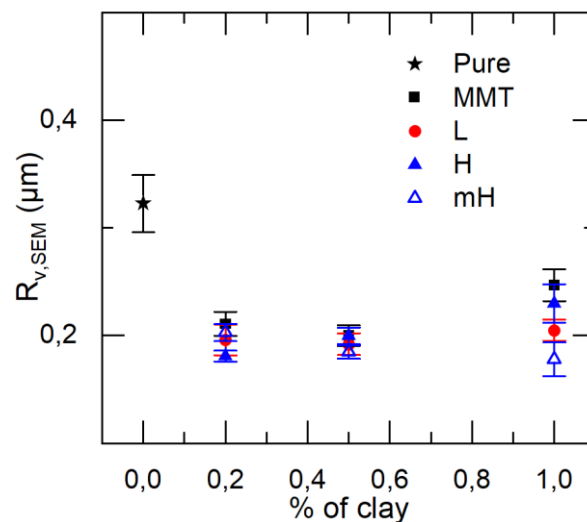


FIG 4 Morphology of PMMA/PS blends with addition of MMT, L, H and mH determined using SEM observations

To understand the effect of the clays on the rheological properties of PMMA in which they are dispersed, small angle oscillatory shear tests were carried out on PMMA nanocomposites to which L, MMT, H and mH were added. Nanocomposites to which 1 % of clay was added were considered since it is the maximum concentration of clay in the PMMA/PS blends. The results are reported in FIG 5. It can be seen that the addition of 1 % of each type of nanoparticles leads to a decrease in the viscosity of the matrix.

This is the author's peer reviewed, accepted manuscript. However, the online version of record will be different from this version once it has been copyedited and typeset.
PLEASE CITE THIS ARTICLE AS DOI: 10.1122/1.5102177

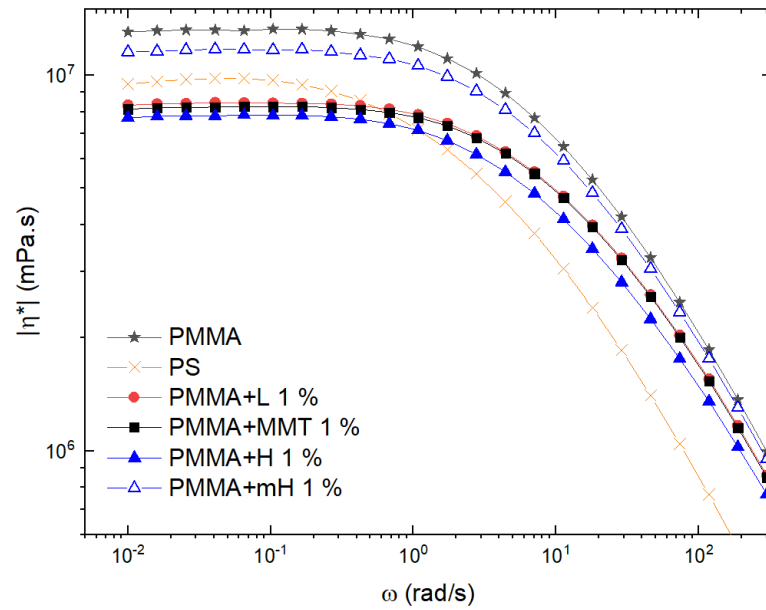


FIG 5 Complex viscosities of PMMA with 1 % of L, MMT, H and mH

TGA was carried out to understand why PMMA viscosity decreases. It was observed that unmodified clays in PMMA led to a faster degradation of PMMA, whereas mH did not (see FIG 6). The degradation of PMMA is enhanced with addition of clays, therefore, leading to lower viscosity.

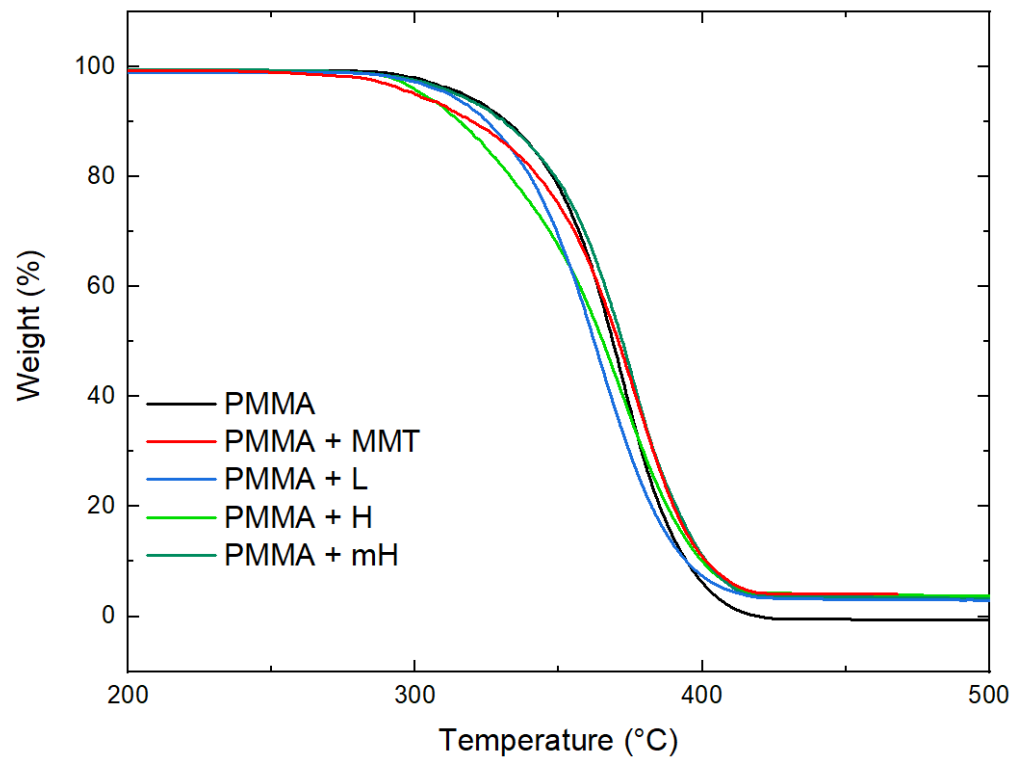


FIG 6 Thermogravimetric analysis of PMMA to which 5 % of MMT, L, H and mH were added

This is the author's peer reviewed, accepted manuscript. However, the online version of record will be different from this version once it has been copyedited and typeset.
PLEASE CITE THIS ARTICLE AS DOI: 10.1122/1.5102177

Because of this decrease of viscosity, the viscosity ratio is modified, which might affect the morphology during processing. As the viscosity of PMMA decreases, the viscosity ratio increases from 0.81 to 1.24. As shown in by Lyu et al. [50] and Caserta et al. [51], coalescence is slowed down when the viscosity ratio of a polymer blend is above 1. According to them, and as the viscosity ratio increases with addition of clays in PMMA, coalescence that may happen during processing could be slowed down, thus leading to smaller droplets in processed samples.

Coalescence tests were carried out following the procedure described in FIG 1 to confirm the theory given above. The relaxation spectra were then calculated from SAOS results at each strain during coalescence. For example, FIG 7 shows the relaxation spectra during coalescence of MMT blends. For each sample at each coalescence strain, the relaxation spectrum shows two relaxations. The fastest one is attributed to the relaxation of the polymer chains of PMMA and PS. The second relaxation, corresponding to the time τ_F , is attributed to the shape relaxation of the droplets after shear. It can be observed that τ_F increases with strain, indicating that the size of the droplets increases and coalescence is happening [42]. The same observations were made for all the blends.

This is the author's peer reviewed, accepted manuscript. However, the online version of record will be different from this version once it has been copyedited and typeset.
PLEASE CITE THIS ARTICLE AS DOI: 10.1122/1.5102177

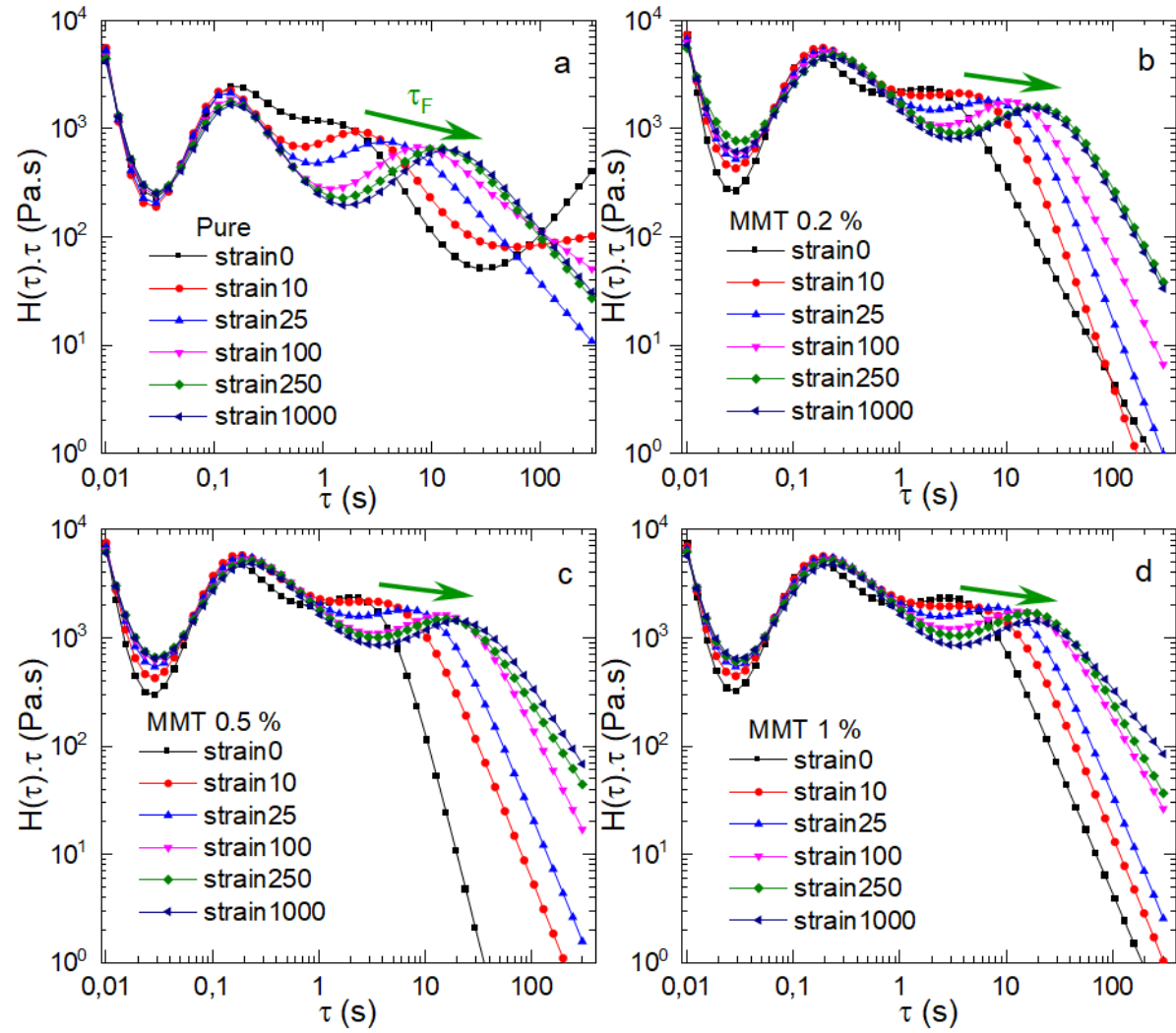


FIG 7 Relaxation spectra of the blends containing (a) 0 %, (b) 0.2 %, (c) 0.5 % and (d) 1 % of MMT during coalescence test

The interfacial tension, α , is calculated at strain = 0 using equation (3). The R_v previously determined by SEM, the viscosities reported in TABLE I and the τ_F determined on the relaxation spectra are used in this equation. The values of α at strain = 0 are reported in TABLE III. It can be noticed that the interfacial tension decreases when clay is added to the blend compared to the pure blend. Knowing that those clays are not located at the interface, it is unclear why the interfacial tension is decreasing. During the coalescence tests, the interfacial tension is considered to be constant. For a more detailed discussion of this assumption, see paper [42].

TABLE III Interfacial tensions between the components of the blends determined using the Palierne model for MMT, L, H and mH blends

% Clay	Pure	MMT			L			H			mH		
	0	0.2	0.5	1	0.2	0.5	1	0.2	0.5	1	0.2	0.5	1

This is the author's peer reviewed, accepted manuscript. However, the online version of record will be different from this version once it has been copyedited and typeset.
PLEASE CITE THIS ARTICLE AS DOI: 10.1122/1.5102177

α (mN/m)	4.3	1.6	1.2	1.2	1.0	1.3	1.0	1.2	1.2	1.4	1.1	1.0	0.9
	± 1.4	± 0.4	± 0.3	± 0.3	± 0.3	± 0.4	± 0.3	± 0.3	± 0.3	± 0.4	± 0.3	± 0.3	± 0.2

Then for each strain, R_v can be determined using the values of α determined at strain = 0 (TABLE III) as well as the τ_F determined on the relaxation spectra in equation (3). FIG 8 compares the coalescence phenomenon using each clay at the highest concentration. Similar evolution of the droplet size as a function of strain can be found in the literature [39]. It can be seen that every clay induces a decrease in coalescence between 40 and 70 %. Coalescence is lessened in the presence of clays but is not completely suppressed which is in agreement with previous results [50], [51]. Also, the results indicate that the smaller the particles the lesser the coalescence.

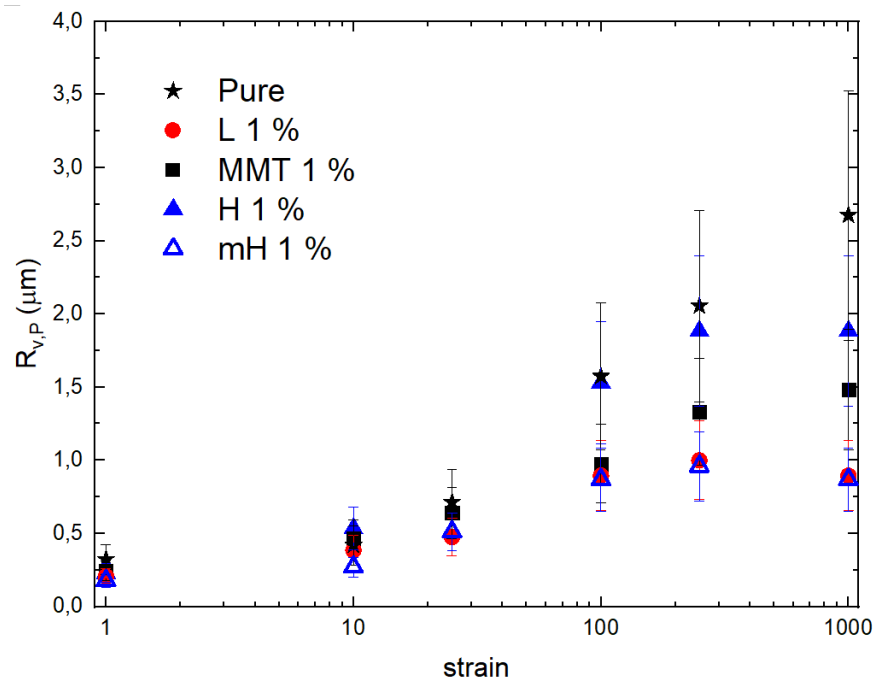


FIG 8 Evolution of $R_{v,p}$ during coalescence tests calculated using the Palierne model for blends to which 1 % of L, MMT and H were added

The morphologies of the samples after coalescence tests were observed by TEM. FIG 9 shows PMMA/PS/mH 1 % blend after the coalescence test. It can be seen that, mH migrated towards the droplets once the droplets got bigger. According to FIG 8, mH starts to stop coalescence at around 100 strain corresponding to a droplet size of 1 μm . As such, they can act as coalescence reducers when the size of the nanoparticles is equal to or larger than the radius of the droplet. Therefore, the size of the nanoparticles have to be chosen carefully because it will greatly influence the size of the droplets during processing. According to those results the smaller the nanoparticles, the smaller the droplets after coalescence.

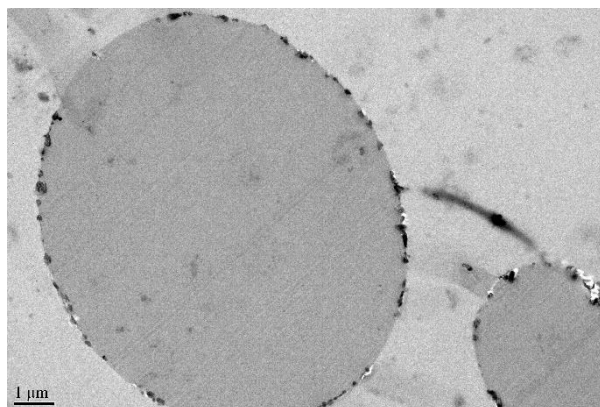


FIG 9 TEM of PMMA/PS blend with 1 % of mH after coalescence experiment

As a conclusion, the reduction of coalescence induced by L, MMT, H and mH, which are located in PMMA, is due to two phenomena: the increase in the viscosity ratio slowing down the coalescence kinetics and the migration of clays towards the interface during shear induced coalescence tests.

2. Effect of location of nanoparticles

The second part of this analysis focusses on the effect of the location of nanoparticles on the morphology and coalescence phenomenon. To do so, three clays were chosen: mL, mMMT and mH as mL is located in the whole blend (FIG 3a), mMMT is located at the interface (FIG 3b) and mH is located in the matrix (FIG 3c).

As seen previously in FIG 3a, b and c, mL is dispersed in the blend with no preferred location, mMMT is located at the interface and mH in the matrix. mH is located in PMMA due to its size larger than the radius of the droplets. The morphology of the blends was observed using SEM and quantified. The radii of the droplets are reported in FIG 10. It can be seen in FIG 10 that the addition of mL did not result in any refinement of the morphology. It is believed to be a consequence of mL small size (30 nm) compared to the size of the droplets (300 nm) and the fact that by being dispersed in the whole blend, mL might not influence significantly any parameter. FIG 10 also shows that mMMT decreases slightly the size of the droplets. Despite its location at the interface it seems that mMMT is less efficient at obtaining smaller droplets than mH after extrusion and before coalescence test. An explanation for that could be that the size (200 nm length) and the rigidity of mMMT does not allow to have smaller droplets, specifically, because it is located at the interface. In other words, the presence of the rigid nano platelets at the interface makes it impossible for the droplet to have a more curved interface, so

it may not be possible to have smaller droplets. That would also explain why the radius increases slightly with the concentration: the more nanoparticles at the interface, the less curvature is possible. Moreover, it can be seen in FIG 3b that the curvature of the droplets is indeed influenced by the presence of mMMT nanoplatelets.

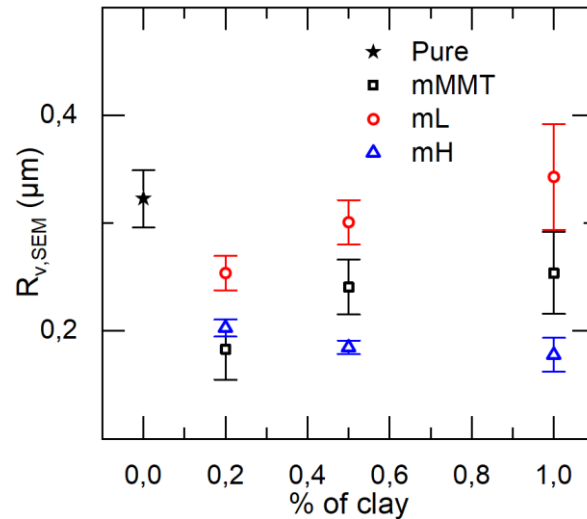


FIG 10 Morphology of PMMA/PS blends with addition of mL, mMMT and mH obtained by SEM observations

Coalescence tests were performed on the blends containing modified clays as well. The values of interfacial tension used are reported in TABLE IV and the results of the test are reported in FIG 11. It can be seen that mMMT is the most efficient at inhibiting coalescence. At a loading of 1 % it completely suppresses coalescence, whereas, mL and mH only decrease coalescence. It should be noted that the influence of mL and mH is similar while their size and location are different.

TABLE IV Interfacial tensions between the component of the blends determined using the Palierne model for mMMT and mL blends

% Clay	Pure	mMMT			mL		
	0	0.2	0.5	1	0.2	0.5	1
α (mN/m)	4.3 ± 1.4	1.6 ± 0.4	1.2 ± 0.3	1.2 ± 0.3	1.0 ± 0.3	1.3 ± 0.4	1.0 ± 0.3

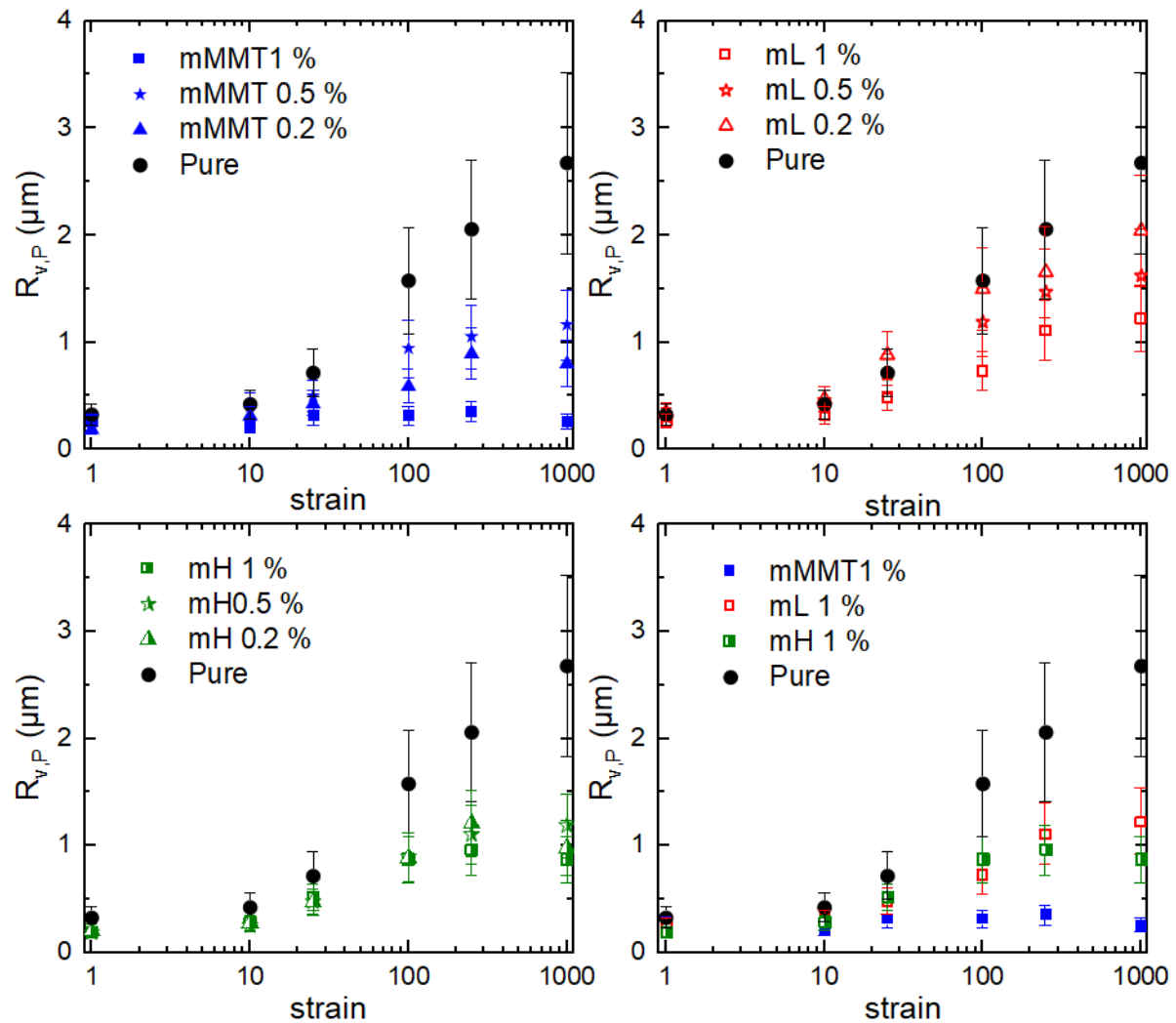


FIG 11 Evolution of $R_{v,P}$ during coalescence tests calculated using the Palierne model for blends containing (a) mL, (b) mMMT, (c) mH and (d) a comparison of the blends containing 1 % of clay

The decrease of coalescence in the case of nanoparticles located at the interface can be explained as follows: either by the barrier effect due to the physical presence of nanoparticles or the Marangoni effect, as explained above. It was shown in Genoyer et al's previous work [40] that the Marangoni effect induced by nanoparticles can be evidenced using relaxation spectra calculated from SAOS tests. In order to check if the relaxation takes longer time the relaxation spectra at higher temperature were obtained (see FIG 12). As was discussed above, the first relaxation is attributed to the relaxation of PMMA and PS chains. The second relaxation corresponds to the relaxation of the droplets after shearing. The third relaxation seen in the case of mL and mMMT (FIG 12a and FIG 12b) is attributed to the Marangoni effect. Because the Marangoni effect is due to the movement of nanoparticles around the interface, Marangoni's relaxation cannot be observed in the case of mH (FIG 12c) which is dispersed exclusively in PMMA.

As FIG 12 shows, there is a Marangoni's relaxation in the case of mL, it can be deduced that enough mL is located at the interface to induce a Marangoni effect. The blend containing 1 % of mL does not display this relaxation, probably, because it is overlaid with the droplets' relaxation. On the contrary, the blend with 0.2 % of mMMT does not display Marangoni's relaxation because it is too long to be detected in the available time range. It can be noticed that Marangoni's relaxation is faster for smaller nanoparticles but a fast Marangoni effect is not enough to ensure coalescence inhibition. The nanoparticles must also be big enough or numerous enough to induce enough barrier effect, the same way a block copolymer as a compatibilizer needs to induce enough steric hindrance to be efficient [42].

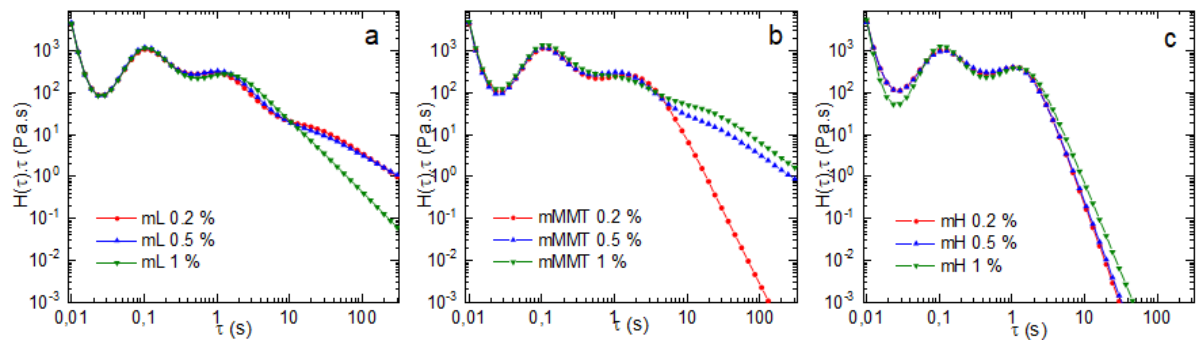


FIG 12 Relaxation spectra of blends at 220 °C with different concentration of (a) mMMT, (b) mL and (c) mH

C. Conclusion

This work presented the effect of the addition of clay particles on the morphology and coalescence of dispersed phase in PMMA/PS blends. Two main factors were studied: the effect of particle size, when dispersed within the matrix, and the effect of the particle location. The main results are reported in TABLE V.

First, the effect of the addition of four different clays: laponite, montmorillonite, halloysite and modified halloysite, (L, MMT, H, mH) with different particle sizes, but all located within the matrix, was studied. It was shown that the presence of clays lead to a refinement of morphology after processing due to a reduction of dispersed phase coalescence originated by an increase the viscosity ratio and migration of particles to the interface. The investigation of the effect of addition of L, MMT, H and mH on the coalescence phenomenon also showed that, the smaller the nanoparticle, the lesser the coalescence. Depending on the ratio between the sizes of the droplets and the ones of the nanoparticles, the migration to the interface induced or impeded coalescence. Of course, the smaller the droplets, the smaller the nanoparticles need to be to locate at the interface.

The second part of the discussion focused on the effect of location of the nanoparticles. Three clays were used for that purpose, modified laponite (mL), which was dispersed in the whole blend without distinction, modified montmorillonite (mMMT), which was located at the interface, and modified halloysite (mH), which was located within the matrix. Contrary to mMMT and mH, mL did not result in a decrease in the droplet size upon addition of clay after processing. mMMT was less efficient at reducing the droplet's size than mH. Indeed, the geometry and rigidity of mMMT makes it impossible for the droplets curvature to increase, therefore preventing the reduction of the droplets size. However, mMMT is more efficient at inhibiting coalescence than both mL and mH because it combines adequate Marangoni and barrier effects. mL is the least efficient clay because it is not in a sufficient concentration to cover the interface and, therefore, to induce any barrier effect, and it is not in a sufficient concentration in the matrix to induce an effect similar to mH as well.

TABLE V Summary of the mechanism of reduction of coalescence induced by the clays of this study

Clay	Size of particle	Location	Coalescence reduction/inhibition mechanism
mMMT	$\approx R_v$	interface	Marangoni effect + barrier effect
mL	$0.1R_v$	everywhere	Marangoni effect only
L, MMT, H & mH	$\gg R_v$	matrix	Increase of the viscosity ratio and migration of particles to the interface

Supplementary Material

See supplementary material for Fourier Transform Infrared spectra and X-Ray diffraction results of modified clays, as well as the droplets size distribution of all blends after processing.

Acknowledgements

Financial supports from the Natural Sciences and Engineering Research Council of Canada (NSERC) and Ecole de Technologie Supérieure (ETS) are gratefully acknowledged. The authors are thankful to the Facility for Electron Microscopy Research (FEMR) department of McGill University for some of the TEM pictures and Mazen Samara for reviewing the paper and excellent suggestions.

References

This is the author's peer reviewed, accepted manuscript. However, the online version of record will be different from this version once it has been copyedited and typeset.
PLEASE CITE THIS ARTICLE AS DOI: 10.1122/1.5102177

- [1] M. Minale, J. Mewis, and P. Moldenaers, “Study of the Morphological Hysteresis in Immiscible Polymer Blends,” *AICHE J.*, vol. 44, no. 4, pp. 943–950, 1998.
- [2] I. Vinckier, P. Moldenaers, a. M. Terracciano, and N. Grizzuti, “Droplet size evolution during coalescence in semiconcentrated model blends,” *AICHE J.*, vol. 44, no. 4, pp. 951–958, Apr. 1998.
- [3] P. V. Van Puyvelde and P. Moldenaers, “Rheology and morphology development in immiscible polymer blends,” *Rheol. Rev.*, pp. 101–145, 2005.
- [4] C. L. Tucker and P. Moldenaers, “Microstructural evolution in polymer blends,” *Annu. Rev. Fluid Mech.*, vol. 34, pp. 177–210, 2002.
- [5] T. Parpaite, B. Otazaghine, A. Taguet, R. Sonnier, a. S. Caro, and J. M. Lopez-Cuesta, “Incorporation of modified Stöber silica nanoparticles in polystyrene/polyamide-6 blends: Coalescence inhibition and modification of the thermal degradation via controlled dispersion at the interface,” *Polymer*, vol. 55, no. 11, pp. 2704–2715, 2014.
- [6] T. Parpaite, B. Otazaghine, A. S. Caro, A. Taguet, R. Sonnier, and J. M. Lopez-Cuesta, “Janus hybrid silica/polymer nanoparticles as effective compatibilizing agents for polystyrene/polyamide-6 melted blends,” *Polymer*, vol. 90, pp. 34–44, 2016.
- [7] M. Huang and H. Guo, “The intriguing ordering and compatibilizing performance of Janus nanoparticles with various shapes and different dividing surface designs in immiscible polymer blends,” *Soft Matter*, vol. 9, no. 30, pp. 7356–7368, 2013.
- [8] M. F. Delbem, T. S. Valera, F. R. Valenzuela-Diaz, and N. R. Demarquette, “Modification of a brazilian smectite clay with different quaternary ammonium salts,” *Quim. Nova*, vol. 33, no. 2, pp. 309–315, 2010.
- [9] G. Cavallaro, G. Lazzara, S. Milioto, F. Parisi, and V. Sanzillo, “Modified halloysite nanotubes: Nanoarchitectures for enhancing the capture of oils from vapor and liquid phases,” *ACS Appl. Mater. Interfaces*, vol. 6, no. 1, pp. 606–612, 2014.
- [10] W. Jinhua *et al.*, “Rapid adsorption of Cr (VI) on modified halloysite nanotubes,” *Desalination*, vol. 259, no. 1–3, pp. 22–28, 2010.
- [11] S. Sinha Ray, S. Pouliot, M. Bousmina, and L. A. Utracki, “Role of organically modified layered silicate as an active interfacial modifier in immiscible polystyrene/polypropylene blends,” *Polymer*, vol. 45, no. 25, pp. 8403–8413, 2004.
- [12] Y. Xi, R. L. Frost, and H. He, “Modification of the surfaces of Wyoming montmorillonite by the cationic surfactants alkyl trimethyl, dialkyl dimethyl, and trialkyl methyl

- ammonium bromides,” *J. Colloid Interface Sci.*, vol. 305, no. 1, pp. 150–158, 2007.
- [13] X. Tang and S. Alavi, “Structure and physical properties of starch/poly vinyl alcohol/laponite RD nanocomposite films,” *J. Agric. Food Chem.*, vol. 60, pp. 1954–1962, 2012.
- [14] B. Wang, M. Zhou, Z. Rozynek, and J. O. Fossum, “Electrorheological properties of organically modified nanolayered laponite: influence of intercalation, adsorption and wettability,” *J. Mater. Chem.*, vol. 19, no. 13, pp. 1816–1828, 2009.
- [15] C. A. Mitchell and R. Krishnamoorti, “Rheological properties of diblock copolymer/layered-silicate nanocomposites,” *J. Polym. Sci. Part B Polym. Phys.*, vol. 40, no. 14, pp. 1434–1443, 2002.
- [16] T. Batista, A. M. Chiorcea-Paquim, A. M. O. Brett, C. C. Schmitt, and M. G. Neumann, “Laponite RD/polystyrenesulfonate nanocomposites obtained by photopolymerization,” *Appl. Clay Sci.*, vol. 53, no. 1, pp. 27–32, 2011.
- [17] K. Yurekli, A. Karim, E. J. Amis, and R. Krishnamoorti, “Influence of layered silicates on the phase-separated morphology of PS-PVME blends,” *Macromolecules*, vol. 36, pp. 7256–7267, 2003.
- [18] E. Joussein, S. Petit, J. Churchman, B. Theng, D. Righi, and B. Delvaux, “Halloysite clay minerals – a review,” *Clay Miner.*, vol. 40, pp. 383–426, 2005.
- [19] Y. Lvov, W. Wang, L. Zhang, and R. Fakhrullin, “Halloysite Clay Nanotubes for Loading and Sustained Release of Functional Compounds,” *Adv. Mater.*, vol. 20, no. 6, pp. 1227–1250, 2015.
- [20] P. Pal, M. K. Kundu, A. Malas, and C. K. Das, “Compatibilizing effect of halloysite nanotubes in polar-nonpolar hybrid system,” *J. Appl. Polym. Sci.*, vol. 131, no. 1, Jan. 2014.
- [21] A. M. C. Souza and N. R. Demarquette, “Influence of coalescence and interfacial tension on the morphology of PP / HDPE compatibilized blends,” *Polymer*, vol. 43, no. 14, pp. 3959–3967, 2002.
- [22] L. Elias, F. Fenouillot, J.-C. Majesté, and P. Cassagnau, “Morphology and rheology of immiscible polymer blends filled with silica nanoparticles,” *Polymer*, vol. 48, pp. 6029–6040, 2007.
- [23] U. Sundararaj and C. W. Macosko, “Drop breakup and coalescence in polymer blends : The effects of concentration and compatibilization,” *Macromolecules*, vol. 28, no. 8, pp. 2647–2657, 1995.

- [24] A. J. Ramic, J. C. Stehlin, S. D. Hudson, A. M. Jamieson, and I. Manas-Zloczower, "Influence of block copolymer on droplet breakup and coalescence in model immiscible polymer blends," *Macromolecules*, vol. 33, no. 2, pp. 371–374, 2000.
- [25] J. Huitric, M. Moan, P. J. Carreau, and N. Dufaure, "Effect of reactive compatibilization on droplet coalescence in shear flow," *J. Nonnewton. Fluid Mech.*, vol. 145, no. 2–3, pp. 139–149, Sep. 2007.
- [26] S. Lyu, T. D. Jones, F. S. Bates, and C. W. Macosko, "Role of block copolymers on suppression of droplet coalescence," *Macromolecules*, vol. 35, no. 20, pp. 7845–7855, 2002.
- [27] J. Vermant, G. Cioccolo, K. Golapan Nair, and P. Moldenaers, "Coalescence suppression in model immiscible polymer blends by nano-sized colloidal particles," *Rheol. Acta*, vol. 43, no. 5, pp. 529–538, 2004.
- [28] A. M. C. de Souza, P. S. Calvão, and N. R. Demarquette, "Linear viscoelastic behavior of compatibilized PMMA/PP blends," *J. Appl. Polym. Sci.*, vol. 129, no. 3, pp. 1280–1289, 2013.
- [29] L. Elias, F. Fenouillot, J. C. Majesté, P. Alcouffe, and P. Cassagnau, "Immiscible polymer blends stabilized with nano-silica particles: Rheology and effective interfacial tension," *Polymer*, vol. 49, no. 20, pp. 4378–4385, 2008.
- [30] A. Taguet, P. Cassagnau, and J.-M. Lopez-Cuesta, "Structuration, selective dispersion and compatibilizing effect of (nano)fillers in polymer blends," *Prog. Polym. Sci.*, vol. 39, no. 8, pp. 1526–1563, 2014.
- [31] P. H. . Macaúbas and N. . Demarquette, "Morphologies and interfacial tensions of immiscible polypropylene/polystyrene blends modified with triblock copolymers," *Polymer*, vol. 42, no. 6, pp. 2543–2554, Mar. 2001.
- [32] M. Yee, P. S. Calvão, and N. R. Demarquette, "Rheological behavior of poly(methyl methacrylate)/polystyrene (PMMA/PS) blends with the addition of PMMA-ran-PS," *Rheol. Acta*, vol. 46, no. 5, pp. 653–664, 2007.
- [33] U. Jacobs, M. Fahrländer, J. Winterhalter, and C. Friedrich, "Analysis of Palierne's emulsion model in the case of viscoelastic interfacial properties," *J. Rheol.*, vol. 43, no. 6, pp. 1495–1509, 1999.
- [34] E. Van Hemelrijck, P. Van Puyvelde, S. Velankar, C. W. Macosko, and P. Moldenaers, "Interfacial elasticity and coalescence suppression in compatibilized polymer blends," *J. Rheol.*, vol. 48, no. 1, pp. 143–158, 2003.

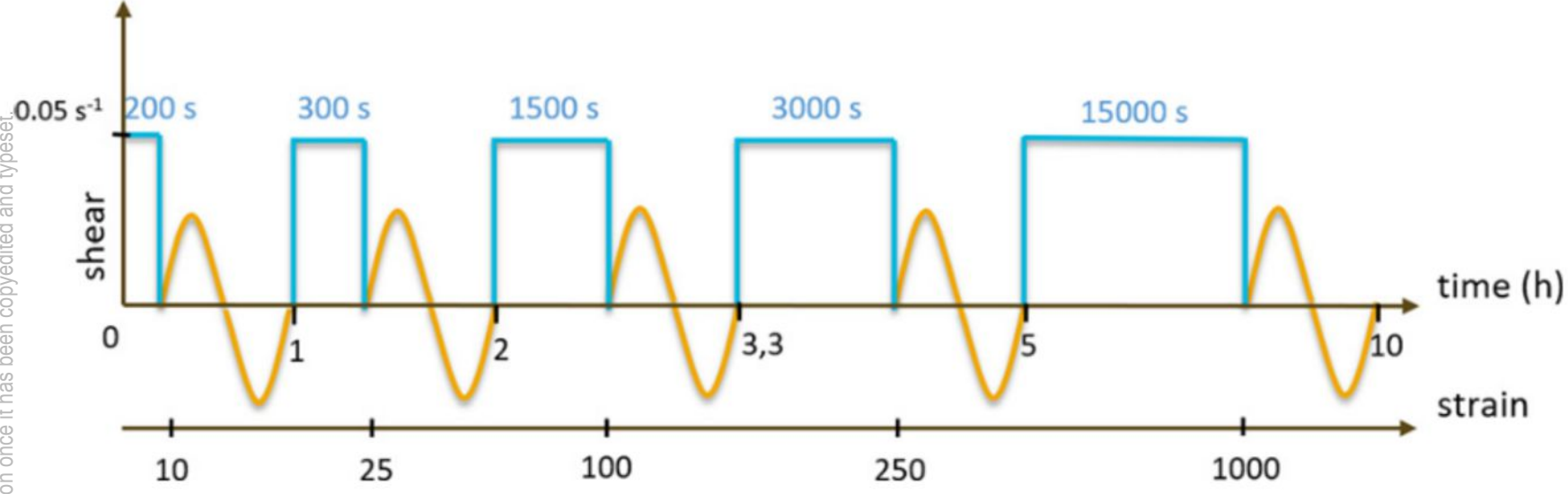
This is the author's peer reviewed, accepted manuscript. However, the online version of record will be different from this version once it has been copyedited and typeset.
PLEASE CITE THIS ARTICLE AS DOI: 10.1122/1.5102177

- [35] E. Van Hemelrijck, P. Van Puyvelde, C. W. Macosko, and P. Moldenaers, “The effect of block copolymer architecture on the coalescence and interfacial elasticity in compatibilized polymer blends,” *J. Rheol.*, vol. 49, no. 3, pp. 783–798, 2005.
- [36] R. Riemann, H. Cantow, and C. Friedrich, “Interpretation of a new interface-governed relaxation process in compatibilized polymer blends,” *Macromolecules*, vol. 30, no. 18, pp. 5476–5484, 1997.
- [37] C. Friedrich and Y. Y. Antonov, “Interfacial relaxation in polymer blends and gibbs elasticity,” *Macromolecules*, vol. 40, no. 4, pp. 1283–1289, 2007.
- [38] I. Fortelný, “An analysis of the origin of coalescence suppression in compatibilized polymer blends,” *Eur. Polym. J.*, vol. 40, no. 9, pp. 2161–2166, 2004.
- [39] P. Van Puyvelde, S. Velankar, J. Mewis, P. Moldenaers, and K. U. Leuven, “Effect of marangoni stresses on the deformation and coalescence in compatibilized immiscible polymer blends,” *Polym. Eng. Sci.*, vol. 42, no. 10, pp. 1956–1964, 2002.
- [40] J. Genoyer, M. Yee, J. Soulestin, and N. Demarquette, “Compatibilization mechanism induced by organoclay in PMMA/PS blends,” *J. Rheol.*, vol. 61, no. 4, pp. 613–626, 2017.
- [41] H. K. Jeon and C. W. Macosko, “Visualization of block copolymer distribution on a sheared drop,” *Polymer*, vol. 44, no. 18, pp. 5381–5386, 2003.
- [42] J. Genoyer, J. Soulestin, and N. R. Demarquette, “Influence of the molar masses on compatibilization mechanism induced by two block copolymers in PMMA/PS blends,” *J. Rheol.*, vol. 62, no. 3, pp. 681–693, 2018.
- [43] D. Graebling, R. Muller, and J. F. Palierne, “Linear viscoelastic behavior of some incompatible polymer blends in the melt. Interpretation of data with a model of emulsion of viscoelastic liquids,” *Macromolecules*, vol. 26, no. 2, pp. 320–329, 1993.
- [44] J. Honerkamp and J. Weese, “A nonlinear regularization method for the calculation of relaxation spectra,” *Rheol. Acta*, vol. 32, no. 1, pp. 65–73, 1993.
- [45] J. F. Palierne, “Linear rheology of viscoelastic emulsions with interfacial tension,” *Rheol. Acta*, vol. 29, no. 3, pp. 204–214, 1990.
- [46] M. Bousmina, P. Bataille, S. Sapiéha, and H. P. Schreiber, “Comparing the effect of corona treatment and block copolymer addition on rheological properties of polystyrene/polyethylene blends,” *J. Rheol.*, vol. 39, no. 3, pp. 499–517, 1995.
- [47] A. J. Paine, “Error Estimates in the Sampling From Particle Size Distributions,” *Part. Part. Syst. Charact.*, vol. 10, no. 1, pp. 26–32, 1993.

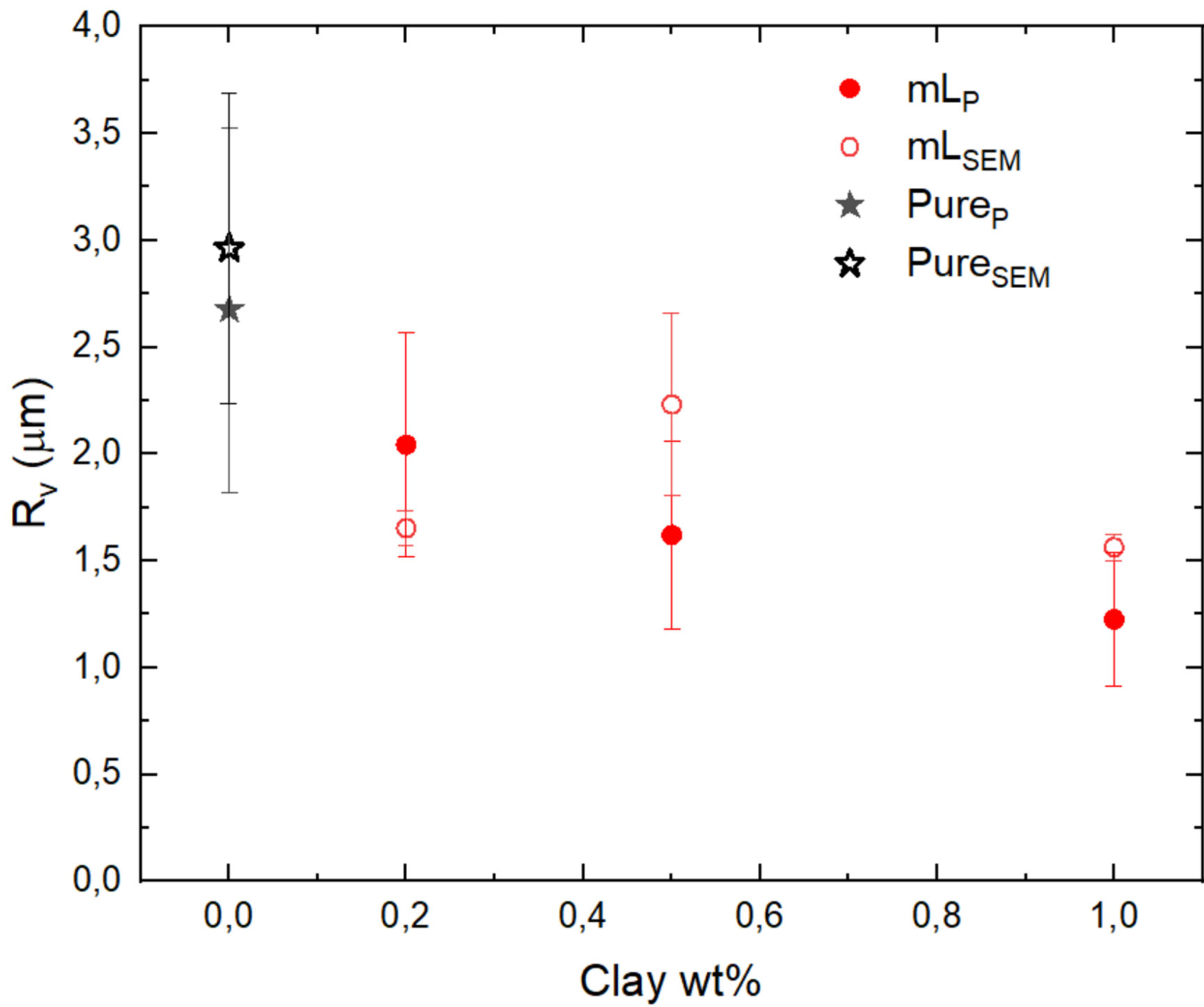
This is the author's peer reviewed, accepted manuscript. However, the online version of record will be different from this version once it has been copyedited and typeset.
PLEASE CITE THIS ARTICLE AS DOI: 10.1122/1.5102177

- [48] S. Caserta, M. Simeone, and S. Guido, “Evolution of drop size distribution of polymer blends under shear flow by optical sectioning,” *Rheol. Acta*, vol. 43, no. 5, pp. 491–501, 2004.
- [49] R. A. de Bruijn, “Deformation and breakup of drops in simple shear flows,” Eindhoven University of Technology, 1989.
- [50] S.-P. Lyu, F. S. Bates, and C. W. Macosko, “Coalescence in polymer blends during shearing,” *AIChE J.*, vol. 46, no. 2, pp. 229–238, 2000.
- [51] S. Caserta, M. Simeone, and S. Guido, “A parameter investigation of shear-induced coalescence in semidilute PIB-PDMS polymer blends: Effects of shear rate, shear stress volume fraction, and viscosity,” *Rheol. Acta*, vol. 45, no. 4, pp. 505–512, 2006.

This is the author's peer reviewed, accepted manuscript. However, the online version of record will be different from this version once it has been copyedited and typeset.
 PLEASE CITE THIS ARTICLE AS DOI: 10.1122/1.5102177

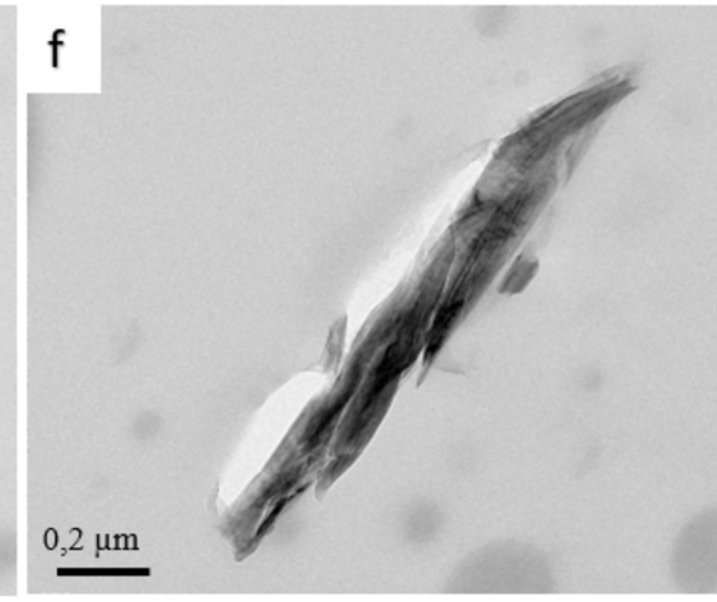
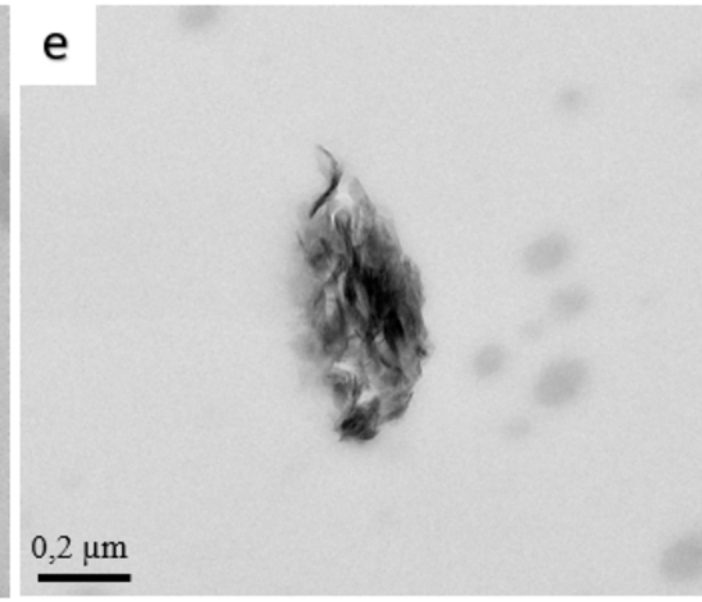
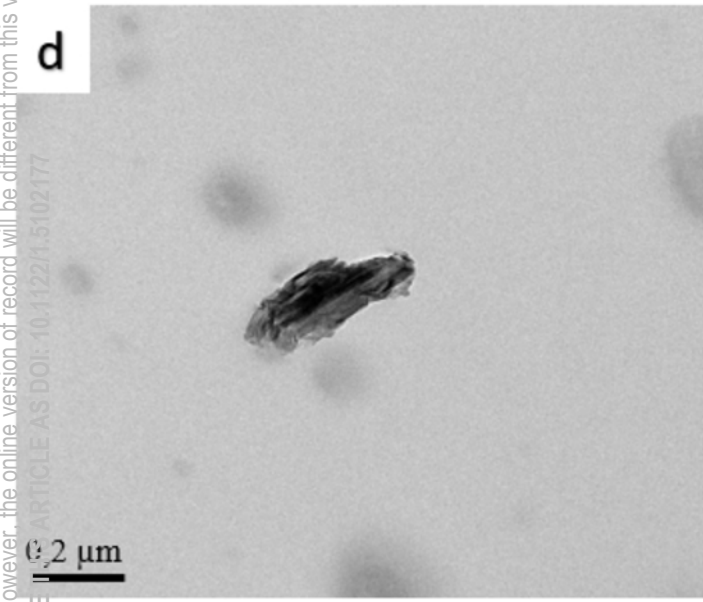
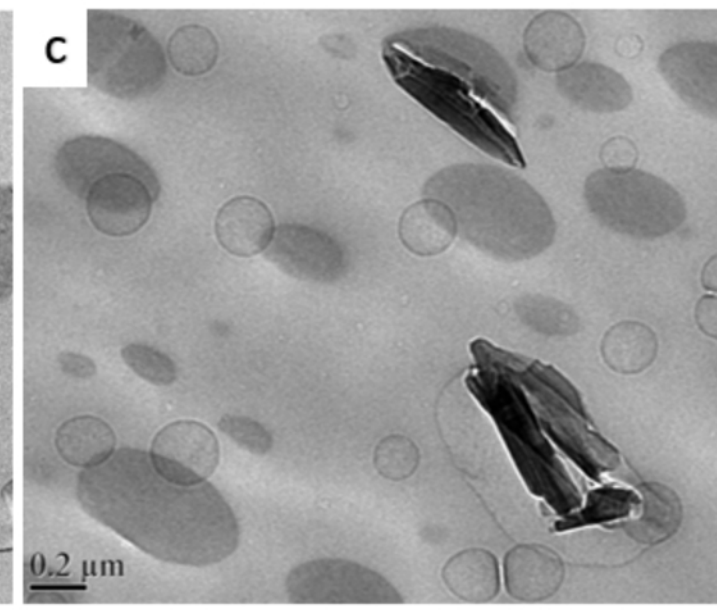
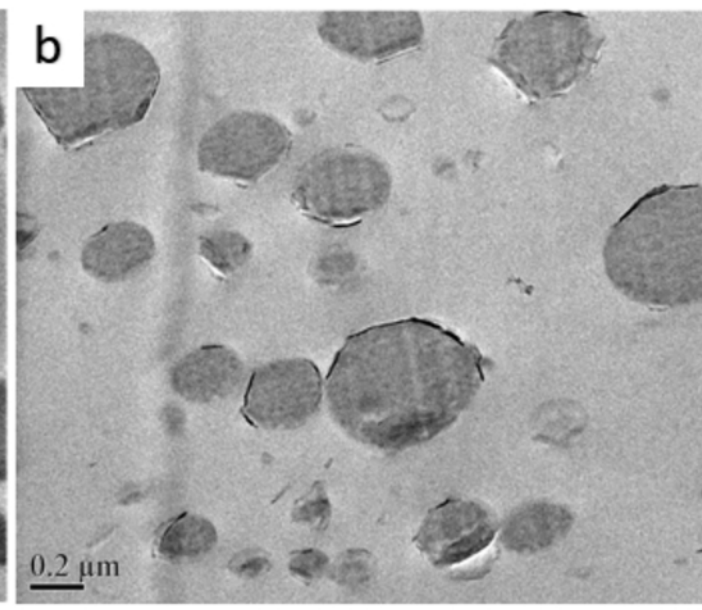
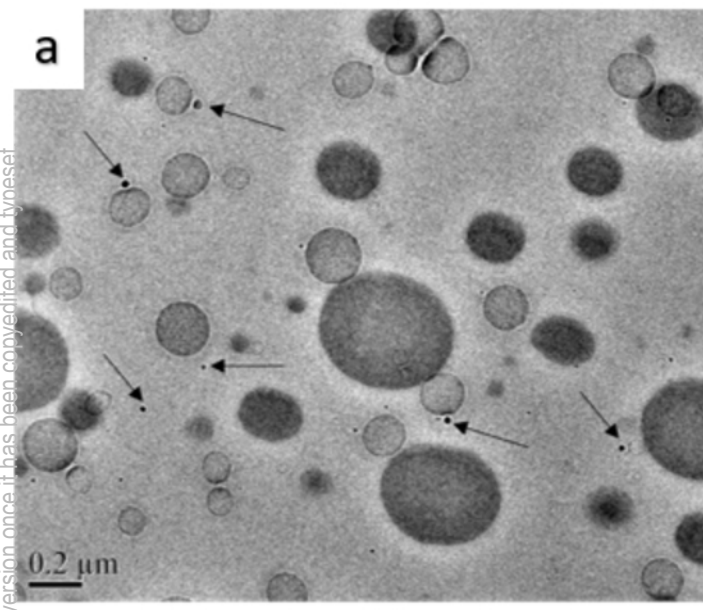


This is the author's peer reviewed, accepted manuscript. However, the online version of record will be different from this version once it has been copyedited and typeset.
PLEASE CITE THIS ARTICLE AS DOI: 10.1122/1.5102177

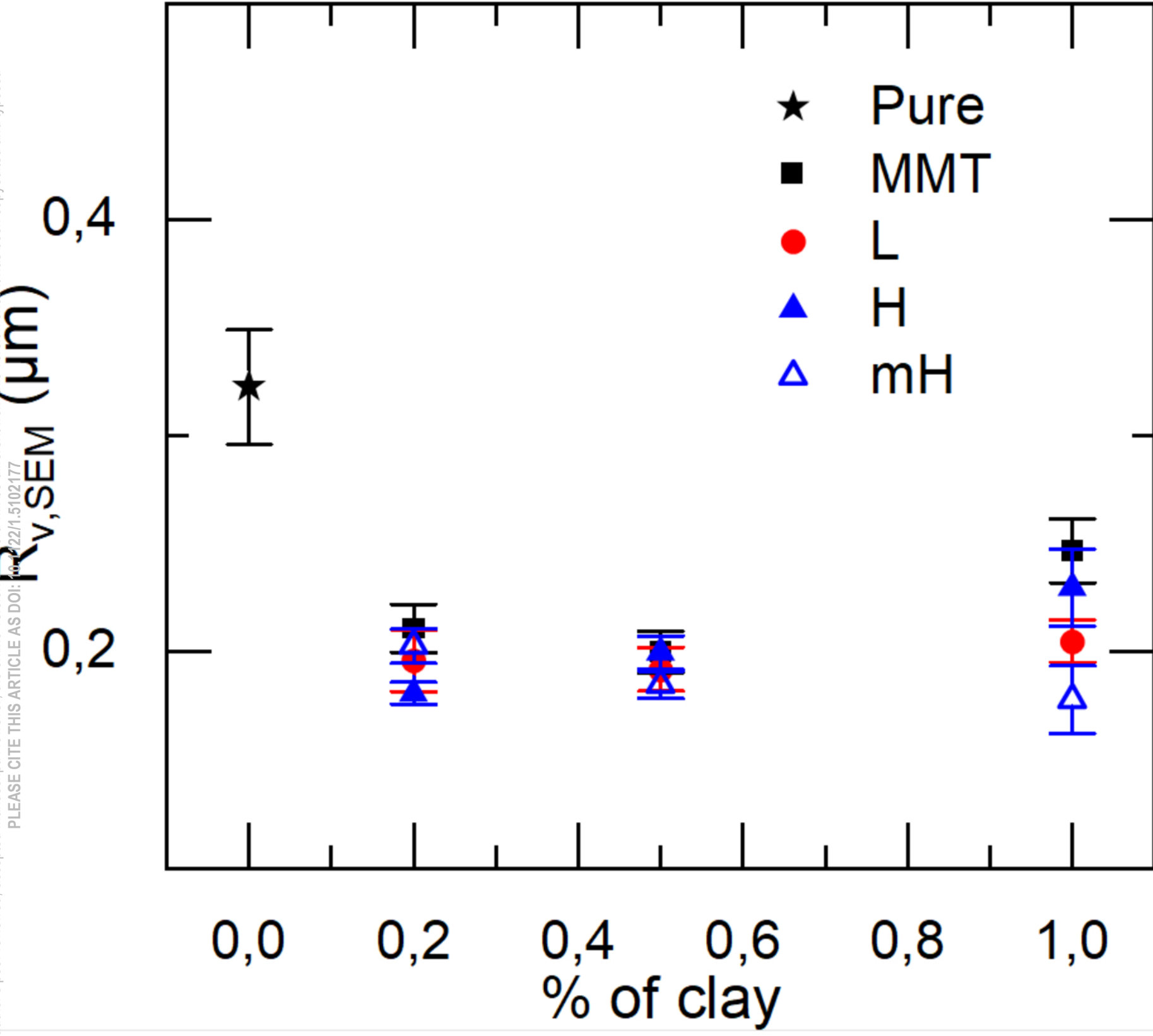


This is the author's peer reviewed, accepted manuscript. However, the online version of record will be different from this version once it has been copyedited and typeset.

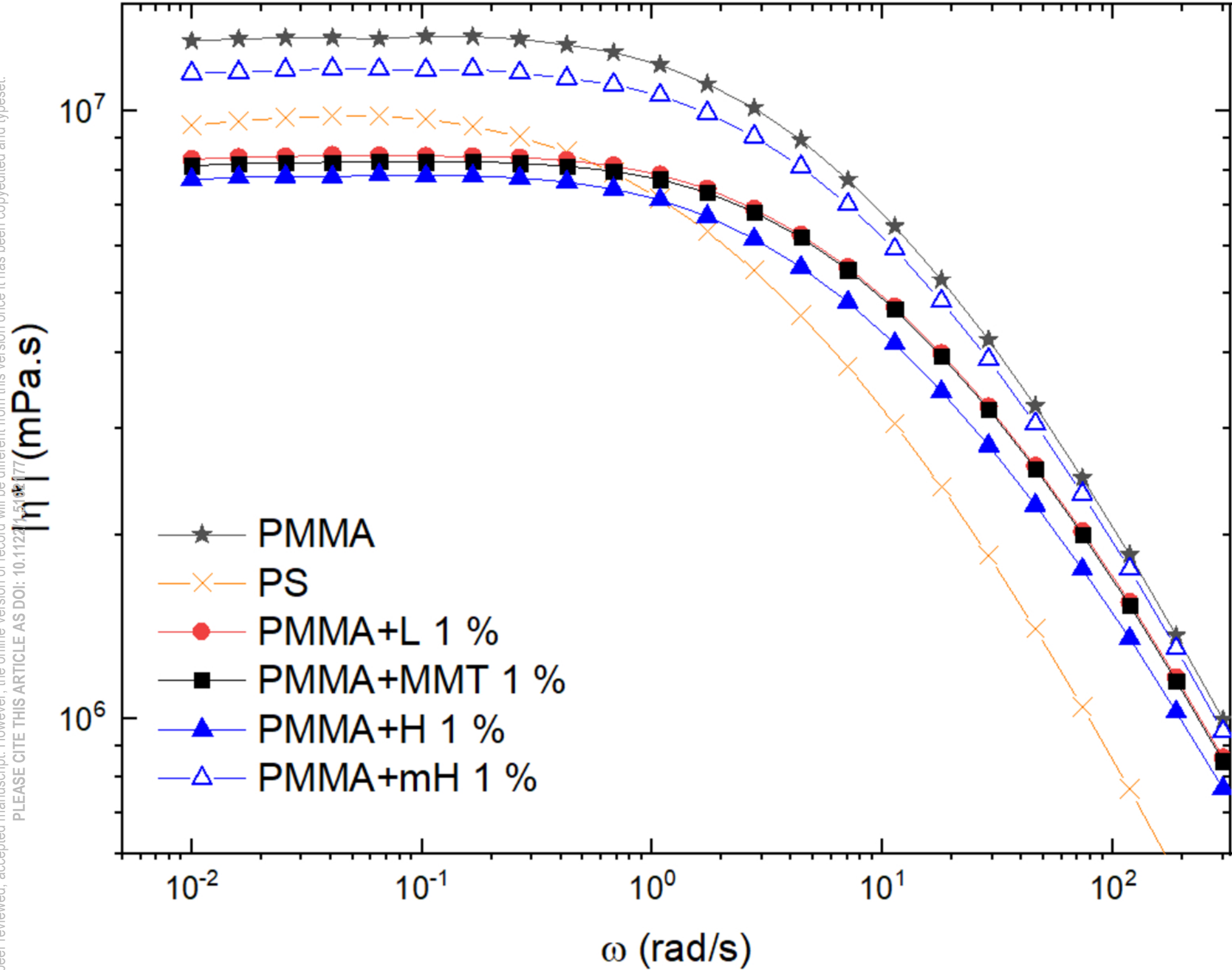
PLEASE CITE THIS ARTICLE AS DOI: 10.1122/1.5102477



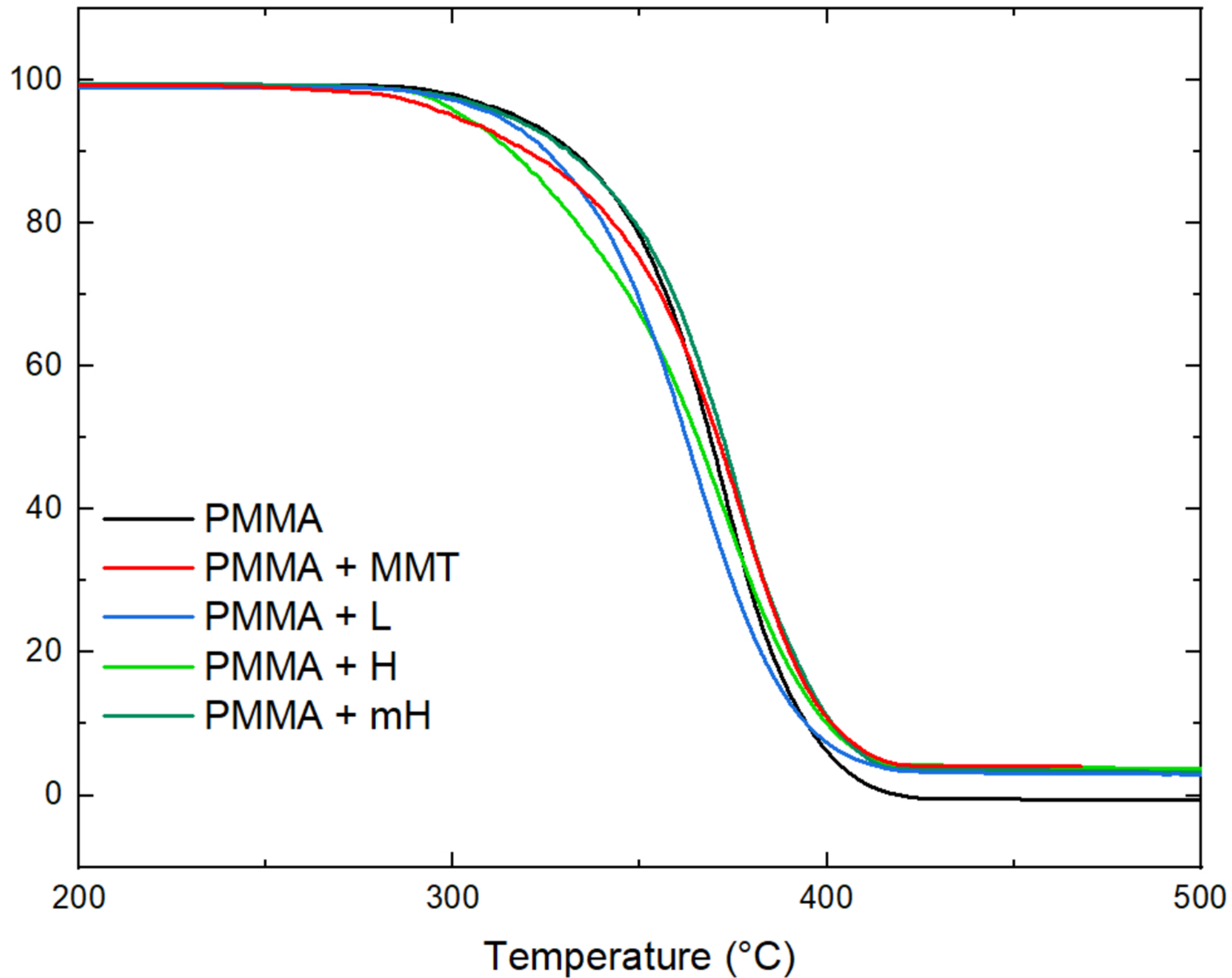
This is the author's peer reviewed, accepted manuscript. However, the online version of record will be different from this version once it has been copyedited and typeset.
 PLEASE CITE THIS ARTICLE AS DOI: 10.1122/1.5102177



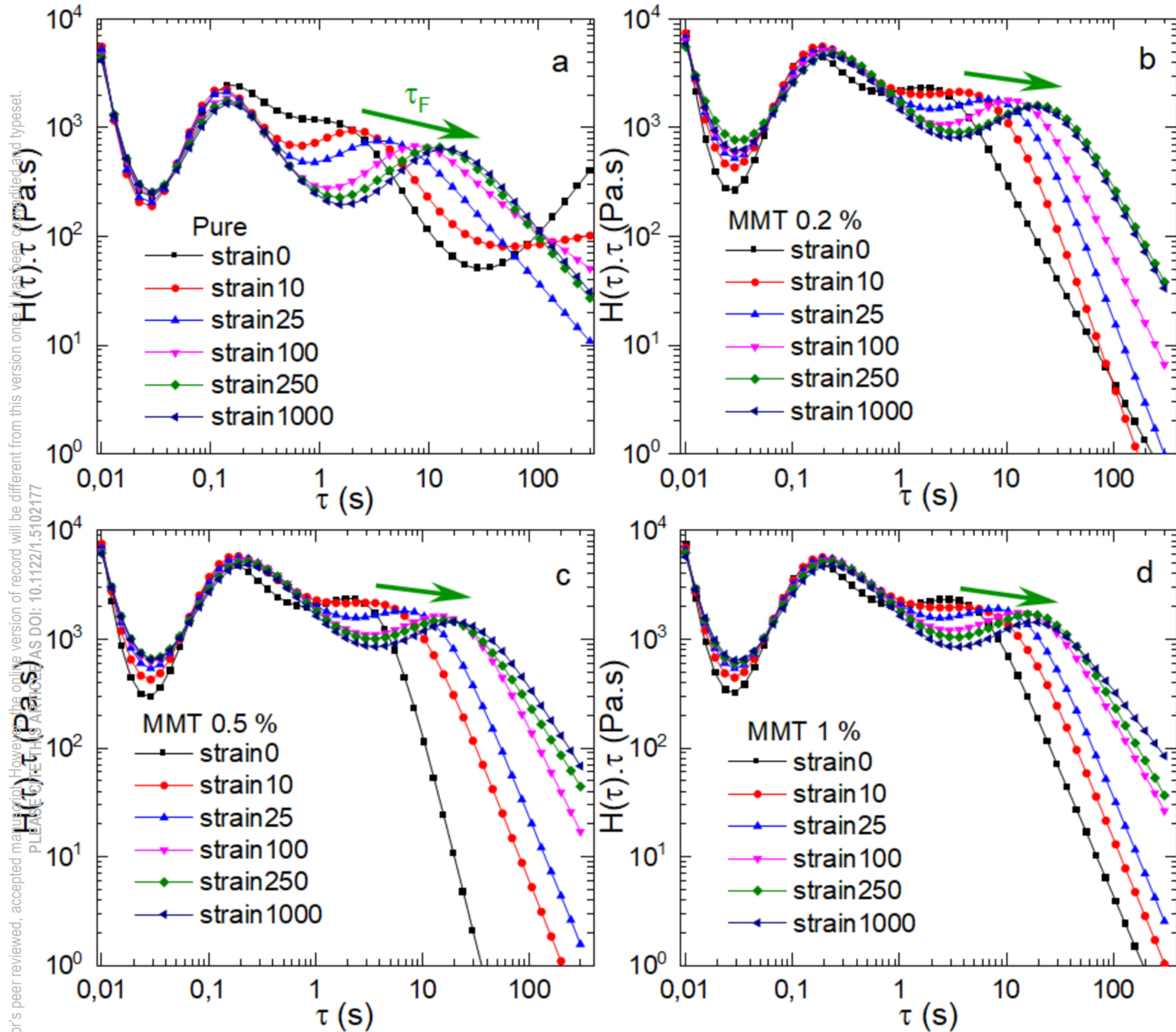
This is the author's peer reviewed, accepted manuscript. However, the online version of record will be different from this version once it has been copyedited and typeset.
 PLEASE CITE THIS ARTICLE AS DOI: 10.1122/1.5102177



This is the author's peer reviewed, accepted manuscript. However, the online version of record will be different from this version once it has been copyedited and typeset.
PLEASE CITE THIS ARTICLE AS DOI: 10.1122/1.5100171



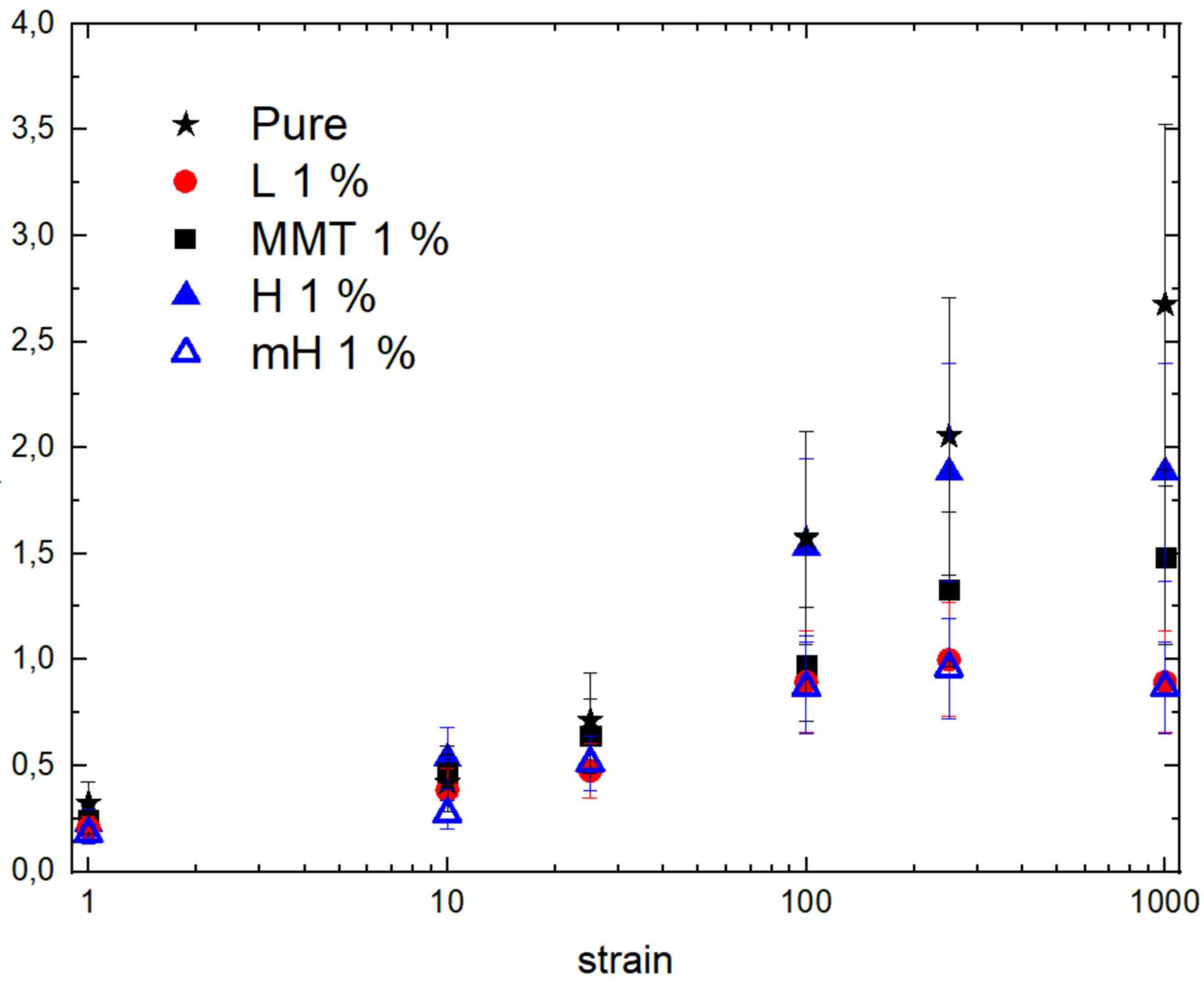
This is the author's peer reviewed, accepted manuscript. However, the online version of record will be different from this version once it has been copyedited and typeset. PLEASE DO NOT DISTRIBUTE OR REPRODUCE THIS MANUSCRIPT AS DOI: 10.1122/1.5102477



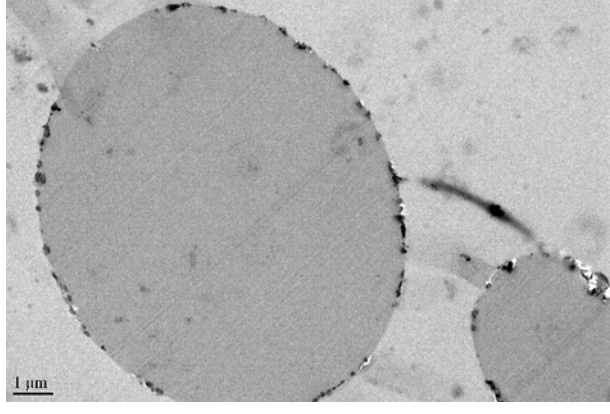
This is the author's peer reviewed, accepted manuscript. However, the online version of record will be different from this version once it has been copyedited and typeset.

PLEASE CITE THIS ARTICLE AS DOI: 10.1122/1.5002177

$R_{V,P}$ (μm)



This is the author's peer reviewed, accepted manuscript. However, the online version of record will be different from this version once it has been copyedited and typeset.
PLEASE CITE THIS ARTICLE AS DOI: 10.1122/1.5102177



This is the author's peer reviewed, accepted manuscript. However, the online version of this record will be different from this version once it has been copyedited and typeset.
PLEASE CITE THIS ARTICLE AS DOI: 10.1122/1.5102477

$K_{V,SEM}$ (μm)

0,4

0,2

0,0

0,2

0,4

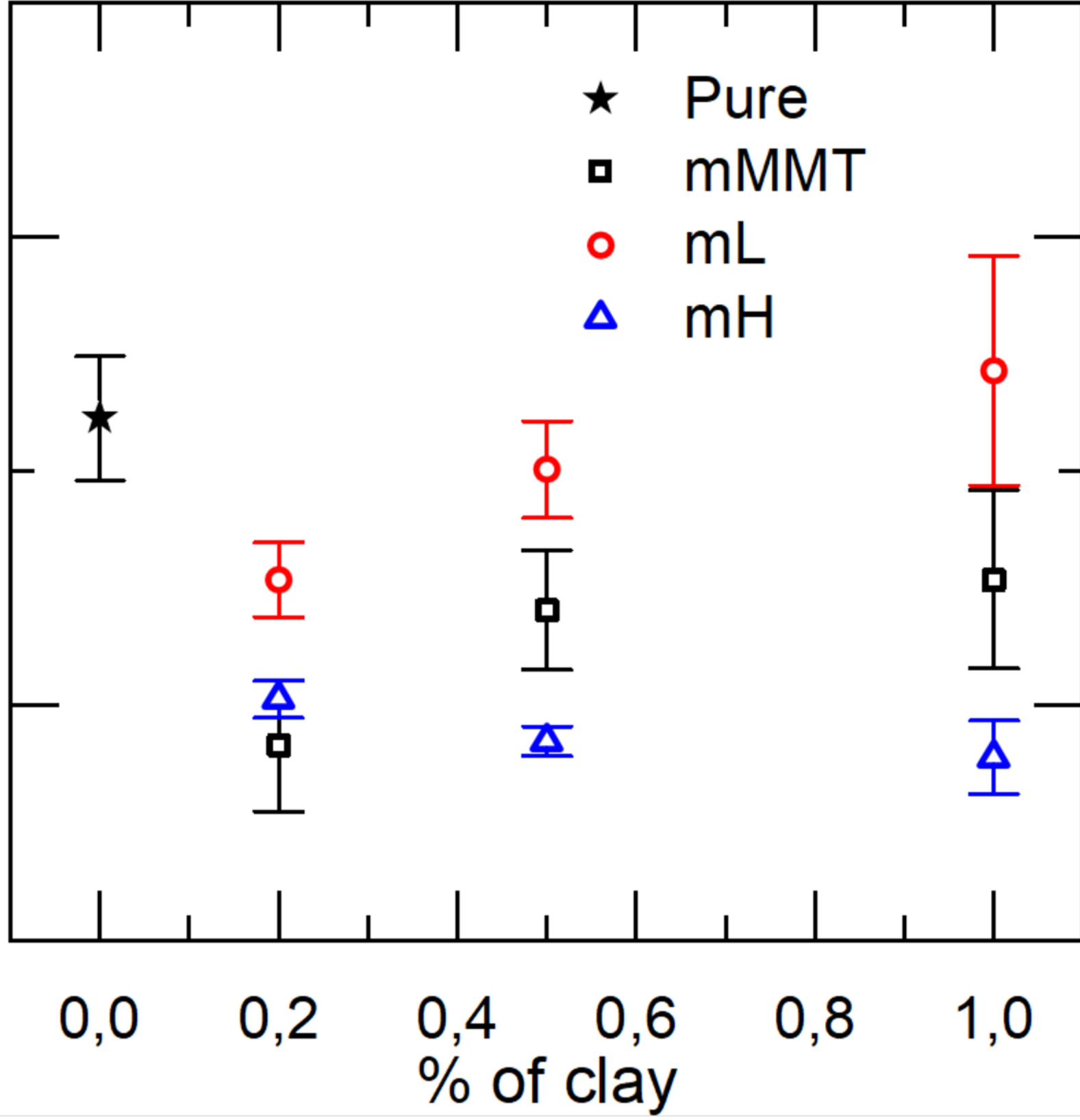
0,6

0,8

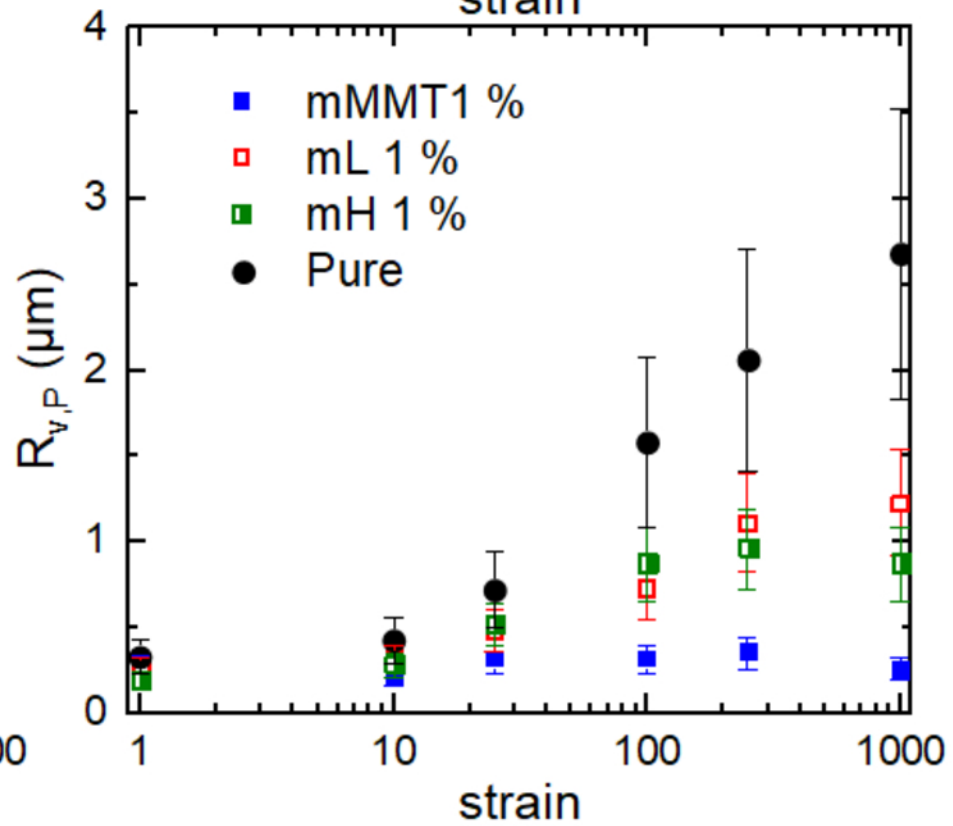
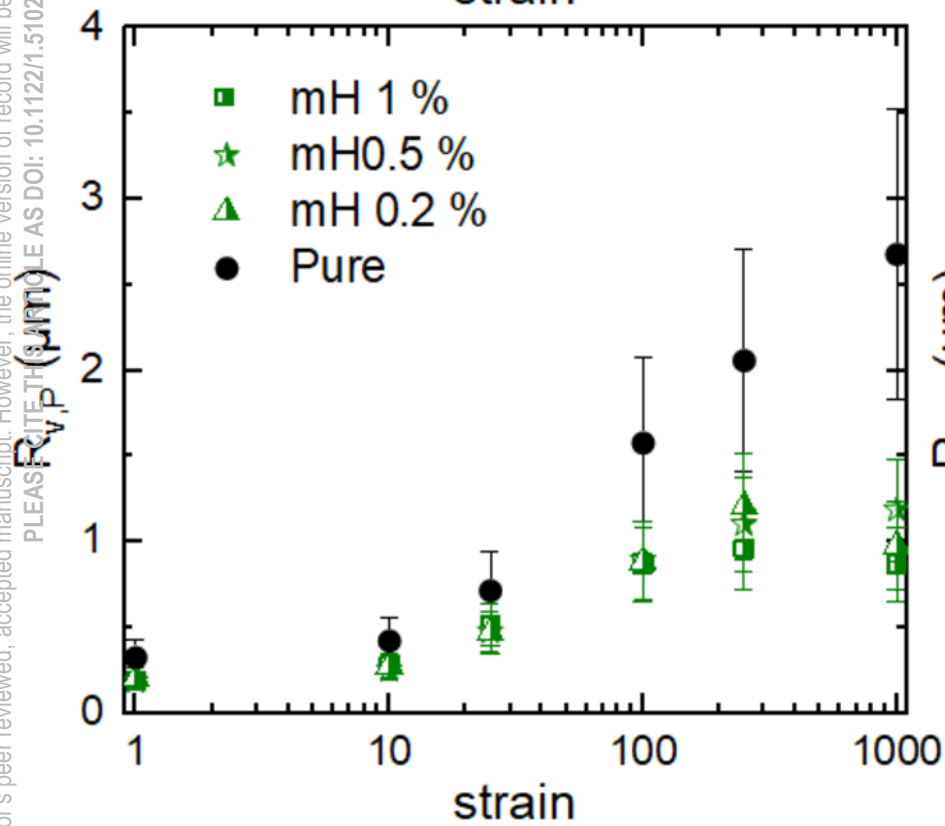
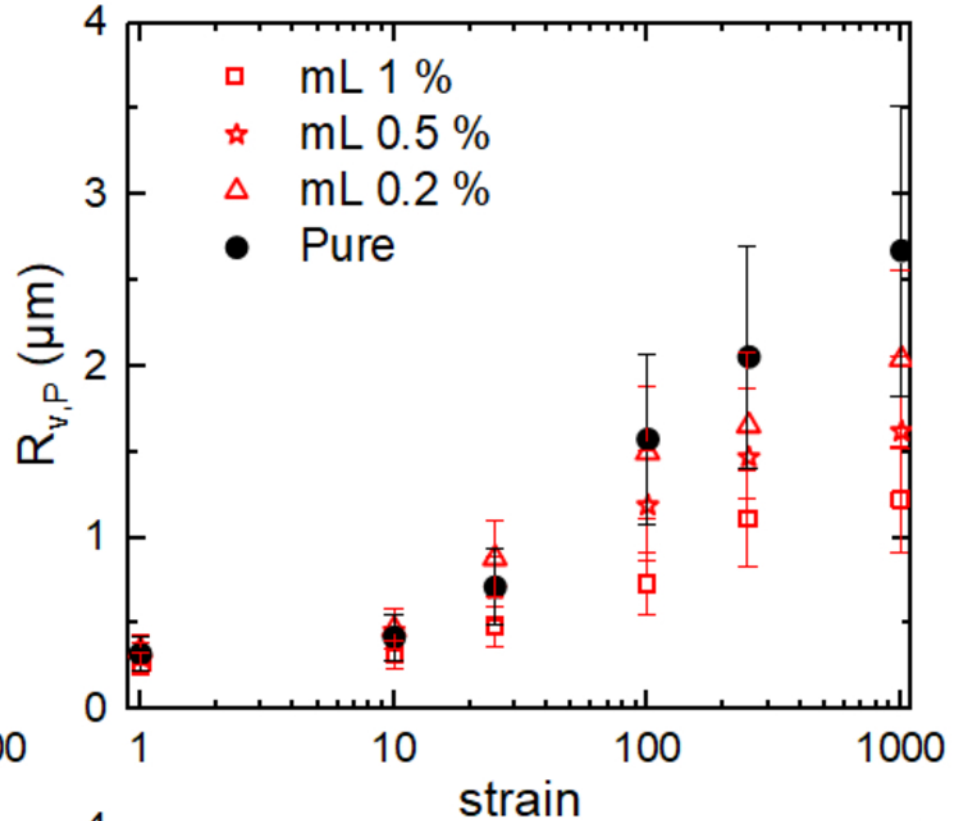
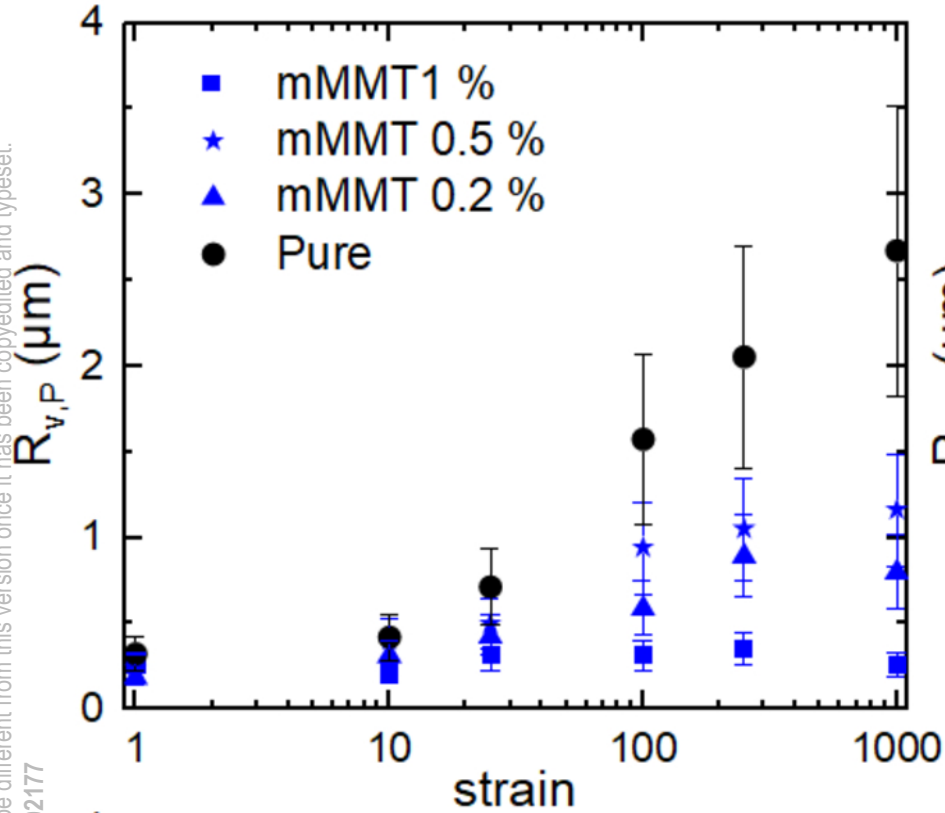
1,0

% of clay

- ★ Pure
- ◻ mMMT
- mL
- △ mH



This is the author's peer reviewed, accepted manuscript. However, the online version of record will be different from this version once it has been copyedited and typeset.
PLEASE CITE THIS ARTICLE AS DOI: 10.1122/1.5102477



This is the author's peer reviewed, accepted manuscript. However, the online version of record will be different from this version once it has been converted and typeset.
PLEASE CITE THIS ARTICLE AS DOI: 10.1122/1.5102177

